aerospace

MDPI

Review

State-of-the-Art DC-DC Converters for Satellite Applications: A Comprehensive Review

Reshma Ravindran * and Ahmed M. Massoud

College of Engineering, Qatar University, Doha P.O. Box 2713, Qatar; ahmed.massoud@qu.edu.qa
* Correspondence: rr2201032@qu.edu.qa

Abstract: Future manned and deep space missions require an Electrical Power System (EPS) that can deliver high power while overcoming challenges like weight and volume constraints and the harsh space environment. A variety of DC-DC converters are employed to supply, store, and transmit power to various satellite subsystems. This paper identifies the design specifications of DC-DC converters for a range of satellite applications and offers a state-of-the-art review of non-isolated, isolated, and integrated topologies. Foreseeing the future of electric propulsion, various sources for electric propulsion are compared, and converters for electric propulsion are studied. The topologies are compared regarding practical parameters like reliability, modularity, redundancy, efficiency, and power density. Furthermore, an application-wise comparison of the topologies and the type of satellite they are suitable for is provided. Finally, the research gaps pertaining to various space applications, such as the design of DC-DC converters, electric propulsion, deep space exploration, electronic component selection, and space-based power satellites, are presented.

Keywords: DC-DC converters; deep space missions; high-power electric propulsion; satellite power system; space applications

check for updates

Academic Editor: Jian Guo

Received: 3 January 2025
Revised: 16 January 2025
Accepted: 16 January 2025
Published: 28 January 2025

Citation: Ravindran, R.; Massoud, A.M. State-of-the-Art DC-DC Converters for Satellite Applications: A Comprehensive Review. *Aerospace* **2025**, *12*, 97. https://doi.org/10.3390/aerospace12020097

Copyright: © 2025 by the authors. Licensee MDPI, Basel, Switzerland. This article is an open access article distributed under the terms and conditions of the Creative Commons Attribution (CC BY) license (https://creativecommons.org/licenses/by/4.0/).

1. Introduction

Satellites have been extensively used for applications such as mobile communication, radio and television broadcasting, military intelligence, weather forecasting, and navigation. The launch of the satellites Sputnik (83 kg) and Explorer 1 (14 kg) by Russia and America, respectively, marked the beginning of the age of satellites [1–3]. Satellites are classified based on their mass into large, medium, and small satellites [1,2]. Large and medium satellites ($Mass > 500$ kg) can carry more payload and integrate larger solar arrays to produce more power, making them suitable for communication, remote sensing, and applications with a lifetime above 10 years. Small satellites ($Mass < 500$ kg) are small and cheap, with shorter mission times than large satellites [1,4,5]. Hence, they are suitable for applications such as Earth observation, disaster management, space science, microgravity research, earthquake forecasting, and gravitational field measurements, to name a few [1,6]. For many applications, two or more small satellites work together to form constellations or operate in formation flying [1,7–9]. The classification of satellites based on their mass, their corresponding power ranges, and applications is demonstrated in Figure 1 [10–16]. The mission's orbit is another parameter to be considered for satellites that are classified based on their relative distance from the Earth as Low Earth Orbit (LEO), Geosynchronous Earth Orbit (GEO), Medium Earth Orbit (MEO), and deep space missions. While LEO satellites are used for remote sensing, GEO satellites are mainly used for communication and broadcasting. MEO satellites are used for navigation, communication, and geodetic/space

environment science [10,17]. The various mission orbits and their relative distances from the Earth's surface are shown in Figure 2.

A bus system and a payload system are the two essential components of a satellite. The elementary operations of the satellite are performed by the bus system, while the mission-specific tasks are performed by the payload system. The EPS is one of the primary and critical components of the bus, contributing to about 33% of the overall mass of the satellite [18,19]. The EPS comprises an energy source, an energy storage unit, and a unit for controlling and distributing power, called the Power Conditioning and Distribution Unit (PCDU) [20]. The solar array is the predominantly used energy source for satellites. The energy storage unit, mostly, Li-ion batteries, ensures a continuous power supply, especially during eclipses or when the solar arrays cannot meet the peak power demand [21]. The PCDU interfaces with the PV array and storage systems or loads, ensuring effective power conditioning and transmission [22]. The EPS is designed based on the time span of the mission, orbit height from the surface of the Earth, solar panel sizing requirements, load demand, satellite mass, radiation effects, efficiency, component count, battery requirements, reliability, redundancy, and fault tolerance level [23,24]. The propulsion system is another crucial component in a satellite, as it enables formation flying, interplanetary paths, collision avoidance, orbital maneuvering, station keeping, and orbit transfers [25,26]. Electric propulsion (EP) has recently gained popularity, especially in small satellites, as it offers better fuel efficiency than the chemical propulsion used in large satellites [27–29]. Better fuel efficiency is guaranteed by a high specific impulse (I_{sp}), which is essentially a measure of the propellant's ability to produce thrust efficiently [30,31]. Nevertheless, EP systems face a variety of challenges. One of the main challenges is the time taken to reach high thrust, which limits their use to specific applications. One solution is to use high-power systems, which improve the time taken to reach high thrust, providing more opportunities for timely orbit changes and interplanetary missions. However, achieving high power without increasing the overall mass or cost is another challenge [25].

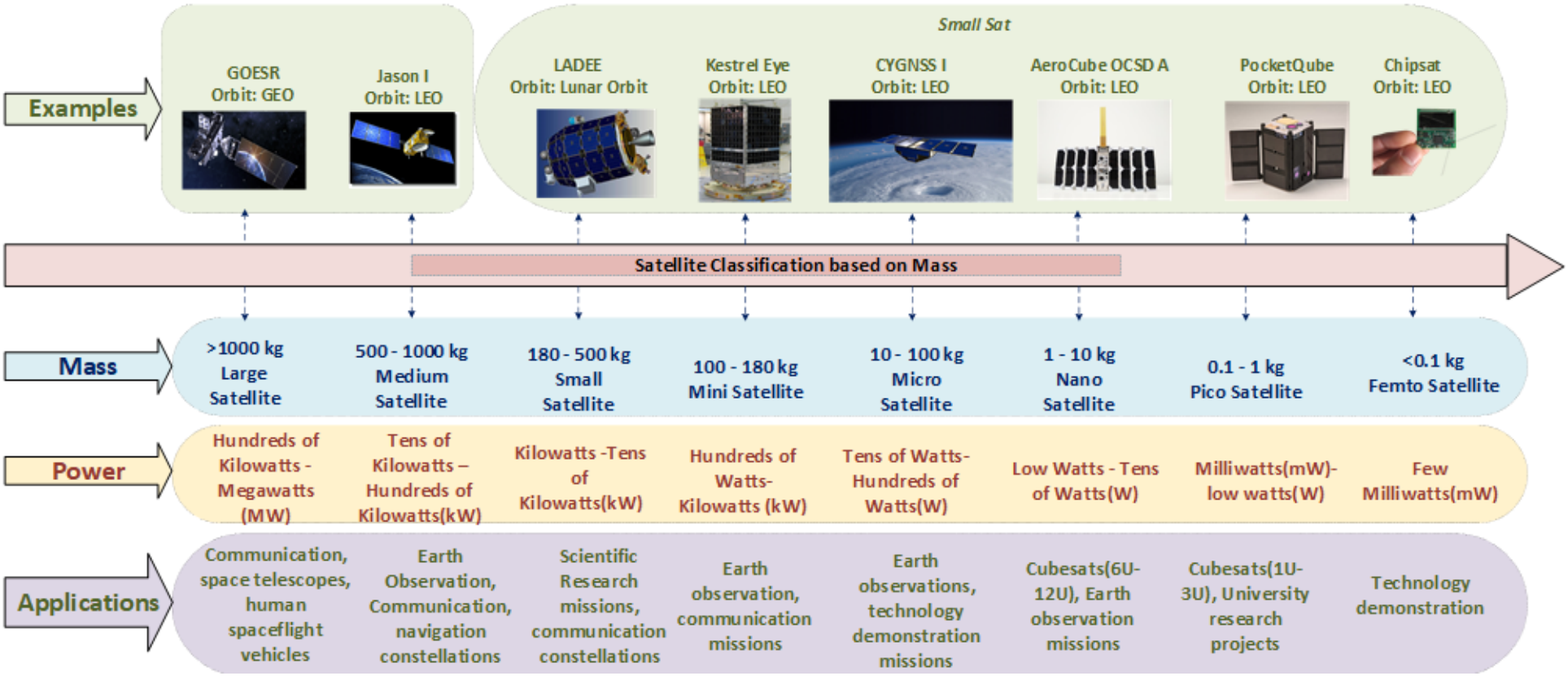

Figure 1. Classification of satellites based on their mass and approximate power levels.

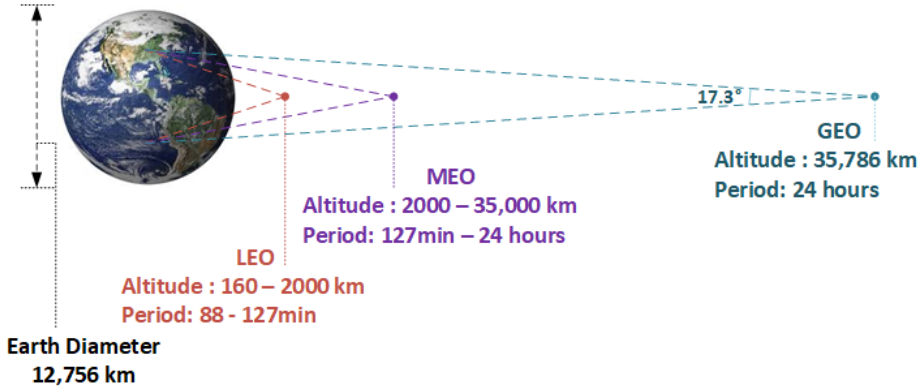

Figure 2. Types of missions and their distances from Earth.

Power electronic converters are critical for generating, transmitting, and storing power in satellites. The power harnessed from solar panels is transformed using a DC-DC converter, stored, and converted for satellite onboard electronics. The power distribution module uses DC-DC converters to regulate the main bus voltage to meet the demands of individual subsystems in the satellite. The battery storage module also needs a DC-DC converter for charge and discharge regulation. Furthermore, isolation may be required at various power conversion phases, depending on the application. Figure 3 shows the various applications of DC-DC converters in satellites. Satellite power designs are driven by increasing power levels while keeping the power system mass and cost within reasonable limits [32]. These demands necessitate power electronic designs capable of managing high distribution currents, thus eventually requiring an increase in the bus voltage (typical voltages are 28 V DC for low-power satellites and 70 V and 100 V DC for larger satellites) to minimize the current and mass of the satellite's EPS [33,34]. Additionally, owing to its benefits, the EP is expected to be a major contributor to propel future deep space and interplanetary missions. This again demands high-power Power Processing Units (PPUs) consisting of highly efficient DC-DC converters for satellite EP systems. Space-level power electronic designs have complex design constraints compared to other commercial applications, as they are exposed to extreme temperatures and radiations. Even though high efficiency and power density are required, reliability is crucial for satellite EPS designs. Moreover, the choice of a DC-DC topology for a given space application is determined by the type of satellite, the orbit, the mission duration, and the power requirements for the mission while adhering to the strict design constraints in space. In this regard, identifying the practical design constraints in space and reviewing the existing literature to compare topologies for various applications based on these constraints becomes essential. A few notable studies in the literature are either limited to a particular type of satellite or mission, or they do not provide comparisons based on practical design constraints in space.

For example, Ref. [35] compared boost-based non-isolated DC-DC converter topologies for satellite MPPT applications. However, the study did not consider other non-isolated or isolated topologies or other applications. Ref. [36] provided a detailed study on small satellite microgrids, where the authors reviewed DC-DC converter topologies, solar arrays, and satellite battery technologies. However, the scope of the study was limited to small satellites, particularly nano-satellites, and did not discuss EP for satellites. This review paper provides an in-depth review of DC-DC topologies for various satellite applications. The scope of this review is not limited to small satellites or Earth-orbiting satellites; it also considers large satellites, interplanetary missions, and deep space missions. This paper spans a wide range of applications of DC-DC converters for satellites. Unlike the existing literature, the topologies are compared using various practical parameters and applications.

The important contributions of this paper are as follows, with a graphical abstract provided in Figure 4:

- We identify the design requirements for DC-DC converters and provide an up-to-date review of various isolated and non-isolated topologies for satellite applications.
- We analyze the scope of EP for future manned and deep space missions and review DC-DC converters for EP in satellites.
- We conduct a performance evaluation of the considered topologies in terms of practical parameters (like reliability, power density, size, efficiency, redundancy, modularity, and performance in harsh environmental conditions) and identify the best topology for a specific satellite application.
- We compare the topologies based on various applications and types of satellites.

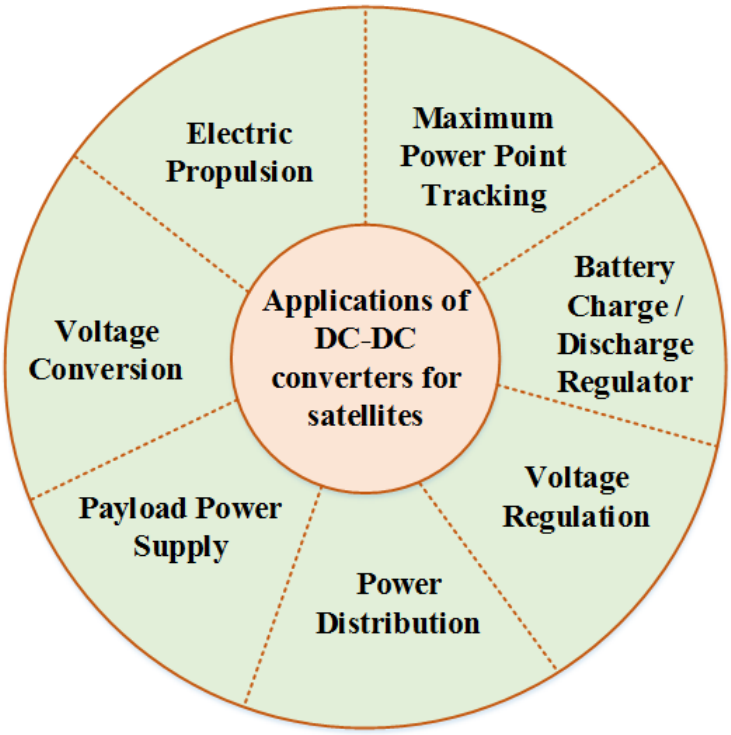

Figure 3. Applications of DC-DC converters for satellites.

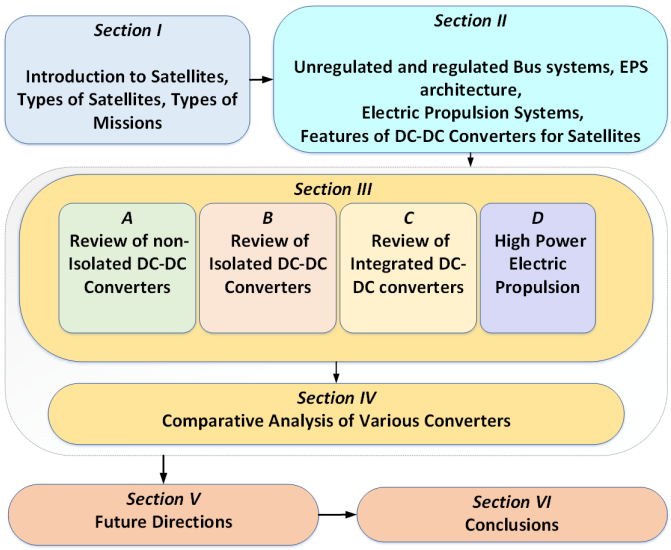

Figure 4. Graphical abstract of this paper.

Given a satellite application, we expect that this paper will guide researchers and the space industry in selecting the best topology. The remainder of this paper is arranged as follows. Section 2 discusses the various electrical subsystems in satellites and the design requirements of DC-DC converters for satellites. Section 3 reviews the various isolated and non-isolated topologies of DC-DC converters, and Section 4 compares them based on practical performance indicators. Section 5 discusses future directions in the area and provides insights into current and future deep space missions. Section 6 concludes this paper.

2. Electrical Subsystems in Satellites

2.1. Unregulated and Regulated Bus Systems for Satellite EPSs and EPS Architectures

Satellite EPSs can be classified into unregulated bus and regulated bus systems. Figure 5a,b show the two types of bus systems [37]. To reduce the number of components, conversion stages, and cost, and to improve the reliability of the regulated bus system, unidirectional and bidirectional converters are sometimes integrated into a single unit, resulting in a three-port integrated converter. A comparison of a conventional two-port converter and an integrated three-port converter for satellite EPSs was discussed in [38]. The power transfer from the source to the batteries and loads uses either the Direct Energy Transfer (DET) or Maximum Power-Point Tracking (MPPT) architectures [23,36,39–46]. Figure 5c,d show these architectures, respectively [47,48]. While the MPPT architecture is used in low- and medium-power LEO satellites and interplanetary missions using unregulated bus systems, the DET is widely used in medium- and high-power GEO satellites using fully regulated bus architectures [49]. Two basic design approaches are used for distributing power: distributed power and decentralized power architectures [50]. Figure 5e shows a schematic of the distributed power architecture, and two types of decentralized approaches are demonstrated in Figure 5f,g [50].

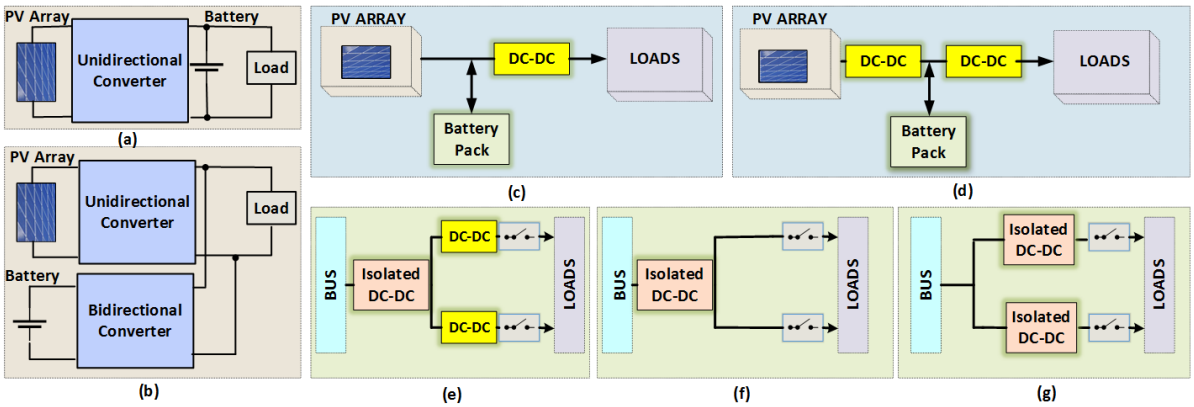

Figure 5. EPS bus systems: (**a**) unregulated and (**b**) regulated EPS architectures for power distribution. (**c**) DET architecture, (**d**) MPPT architecture, (**e**) distributed architecture, (**f**) decentralized architecture with one input and many outputs, (**g**) decentralized architecture with multiple isolated converters.

The DET architecture is a dissipative method that dissipates excess power and regulates the bus voltage [51,52]. One of the most widely used DET architectures is the Sequential Switching Shunt Regulator (S3R) due to its simplicity, high reliability, and efficiency [53]. In the S3R, the PV array is split into several sections, each individually connected to a shunt regulator. A main error amplifier regulates the main bus voltage and controls the power converters: the Battery Charge Regulator (BCR) and the Battery Discharge Regulator (BDR) [54]. A modified S3R, called the Sequential Series Shunt Regulator (S4R), was proposed in [55], which adds another series module to the S3R to improve

its reliability. The MPPT architecture is a series bus transfer method that uses a power converter in series between the PV and loads to maintain bus voltage stability. For MPPT, the algorithms used in stand-alone terrestrial applications, such as the Perturb and Observe (P&O), Incremental Conductance (IC), and Ripple Correlation Control (RCC) methods, may be used. Compared to the IC and RCC methods, the P&O oscillates more and draws less power. More power is extracted using the IC method than the RCC method. In contrast to the IC method, the RCC method is smoother and exhibits fewer oscillations [36]. A detailed comparison of the MPPT algorithms for space applications is provided in [56,57]. S3R and MPPT each offer distinct advantages, so their trade-offs must be carefully considered to make the optimal choice. Moreover, techniques combining the two approaches to leverage their specific advantages are also being studied [52].

2.2. Electrical Propulsion Systems

EP systems for satellite applications convert electrical potential energy to kinetic energy to accelerate a propellant. The transition can generally be done electrostatically, electrothermally, or electromagnetically based on the method used to accelerate the propellant [25,58–60]. In contrast to chemical propulsion, EP relies on energy sources such as solar arrays, batteries, a Radioisotope Thermoelectric Generator (RTG), or a nuclear reactor and accounts for only about 10–50% of the overall mass of a satellite [61,62]. The most popular and mature technology is solar EP. However, the scope of solar EP is limited by the available solar radiation in space, which decreases quadratically with the distance from the sun [63]. Nuclear EP uses energy from a fission reaction to ionize the propellant to generate the required thrust. It can provide higher power than solar EP and is especially beneficial for missions further from the sun, where the ability to harness solar power becomes impractical [64]. Nevertheless, several barriers need to be crossed before its actual implementation. A schematic showing various aspects of electric propulsion, such as the types of electrical thrusters along with their power levels, the scope of solar EP and nuclear EP, and a few past, present, and future solar EP missions along with their power levels, is shown in Figure 6 [65].

A PPU is the core component of the EP system, which offers power conditioning and control for the thrusters for the EP system. The PPU uses DC-DC converters to convert the low-voltage, high-current satellite power into high-voltage, low-current power required by the thruster while providing isolation. The voltage level requirement varies based on the thruster. For instance, while ion thrusters require high voltages in the range of kilovolts, electrothermal thrusters require moderate voltages only. Thus, the PPU must be designed to meet each thruster type's unique electrical and operational demands. Moreover, considering the limited power resources in space, the efficiency and reliability of PPUs are crucial. Thus, efficient power electronic designs are required to ensure that maximum energy is converted into proper thrust. Reliability is achieved through modular and robust designs using specially designed space-grade components [66].

2.3. Features of DC-DC Converters for Satellite Applications

DC-DC converters are crucial components in satellites, and their design affects the overall performance of the satellite. In the era of the miniaturization of satellites, a converter capable of providing high power without increasing the mass or volume of the EPS is highly relevant. In power electronics, improved power density is achieved at high switching frequencies, leading to reduced dimensions of magnetics. Nevertheless, high switching frequency increases switching losses, resulting in larger heat-sink requirements. Thus, a trade-off exists between power density and heat dissipation requirements. Considering the harsh and stringent environmental conditions in space, the converter components must be

carefully chosen to perform well under such conditions. Thus, in summary, the following design requirements are desirable for DC-DC converters in satellite applications [67,68]:

- High power density.
- High efficiency.
- Minimum increase in volume/weight/heat management.
- Reliability.
- Modularity.
- Good performance in harsh environments like large temperature and pressure variations, mechanical vibrations, etc.
- High switching frequency to minimize the size of magnetic components.
- Lower Electromagnetic Interference (EMI).

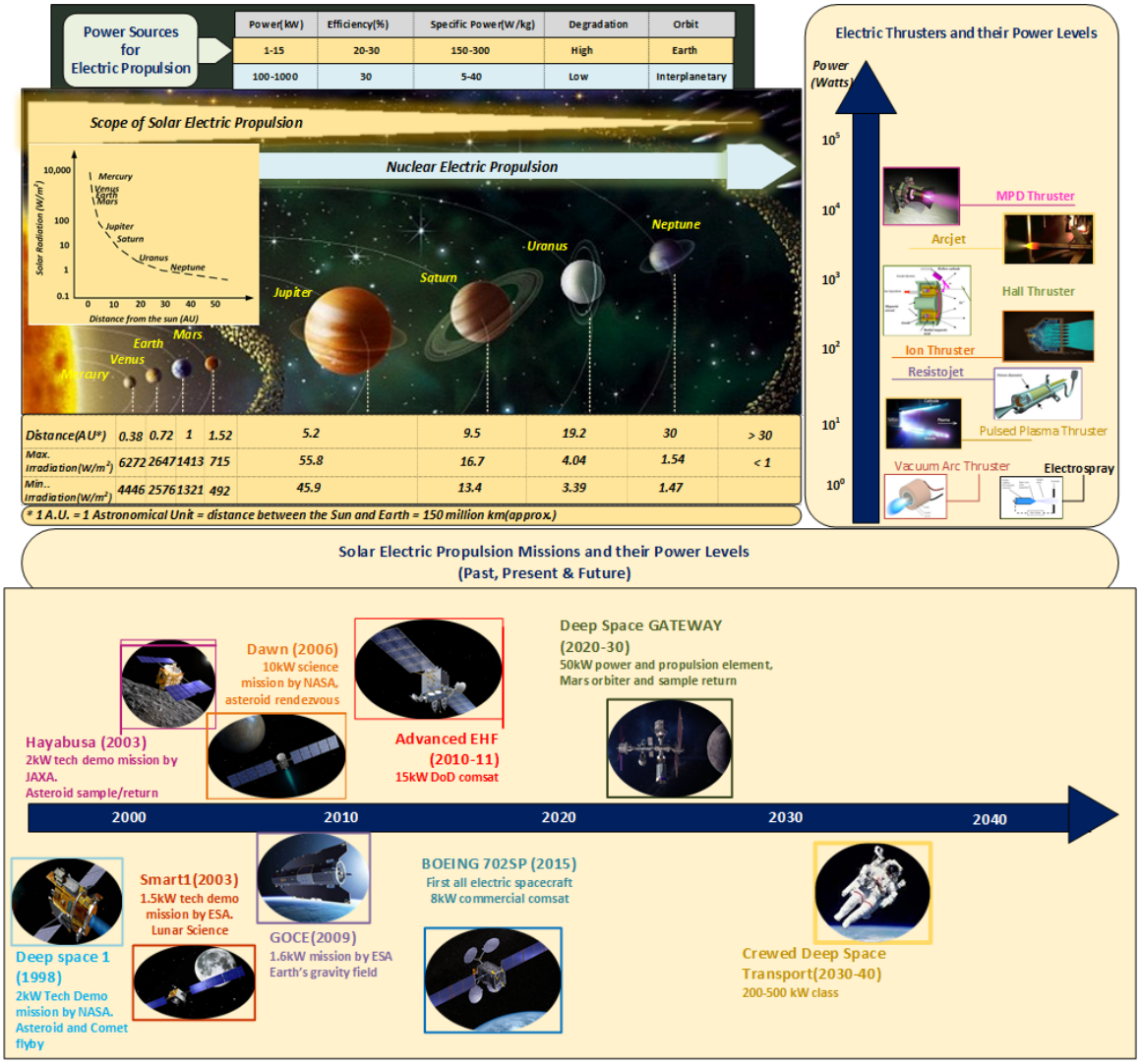

Figure 6. Summary of various aspects of EP (power sources for EP, electric thrusters along with their power levels, and the evolution of solar EP).

These features are schematically represented in Figure 7. Several DC-DC converter topologies are mentioned in the literature for various applications. However, they cannot be directly adopted for satellite applications due to the strict design requirements in space. The following section provides a detailed review of the topologies that can be adopted for satellite applications.

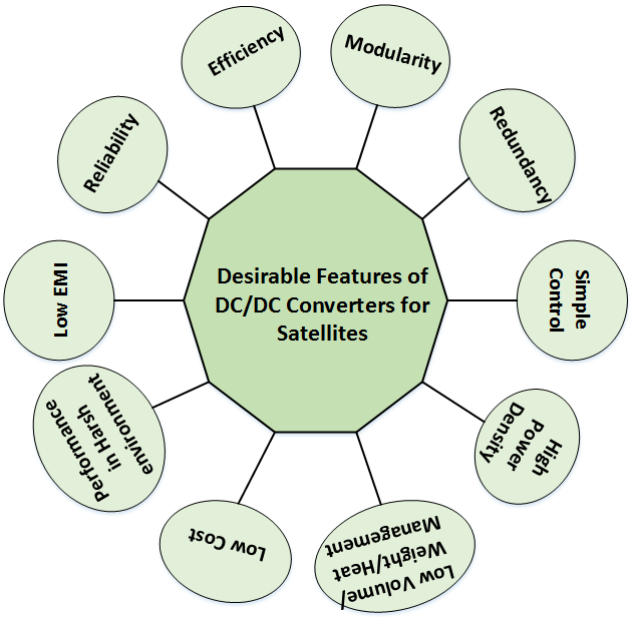

Figure 7. Desirable features of DC-DC converters for satellite applications.

3. Review of DC-DC Converters for Satellites

A review of various DC-DC converters for satellite applications is provided in this section. For this review, the topologies are classified into non-isolated and isolated topologies. Various integrated converters (isolated and non-isolated) and topologies for high-power EP are also presented.

3.1. Non-Isolated Topologies

This section reviews the various non-isolated DC-DC converters for satellite applications. The classification is shown in Figure 8. Non-isolated converters provide benefits such as design simplicity, reliability, and a reduced component count [69]. Nevertheless, they suffer from problems such as a lack of controllability and increased losses due to extreme duty-cycle operation [70]. They find applications in small satellites for converting and regulating power.

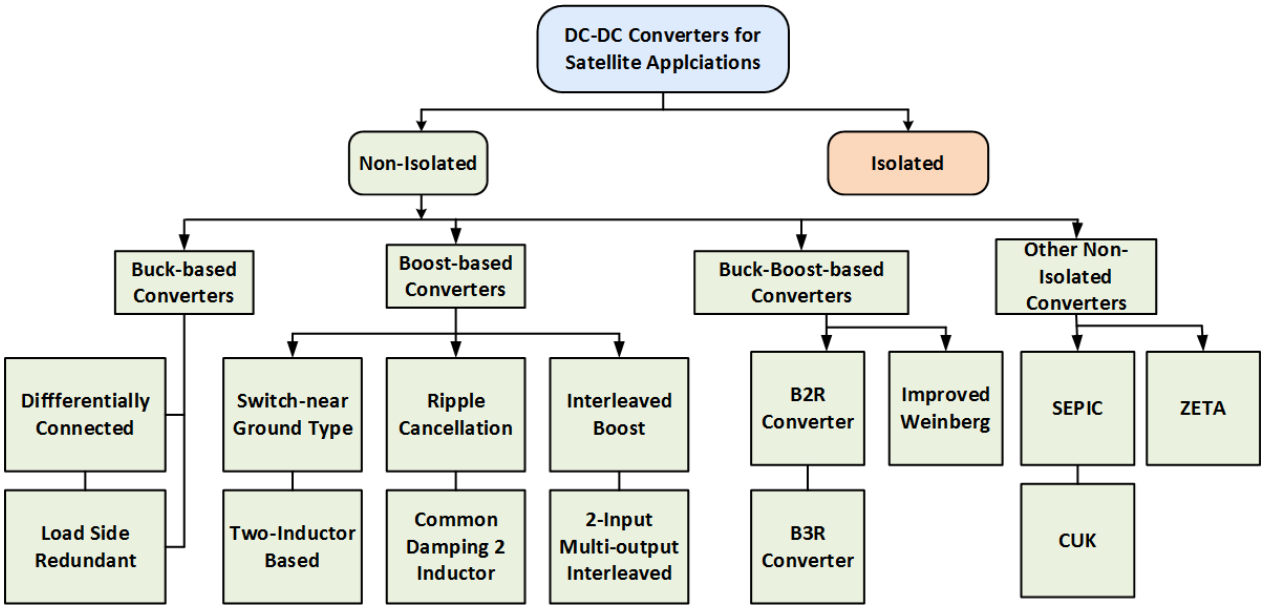

Figure 8. Classification of non-isolated DC-DC converters for satellite applications.

3.1.1. Buck-Derived Topologies

Buck converters are extensively used in small satellites to lower the main bus voltage to power the LV subsystems in the satellite. In [71], a buck converter was used for an educational nano-satellite to step down the bus voltage from 16.8 V to 12 V, 5 V, and 3.3 V to supply the loads. Another demonstration was provided in [72], where a 5 V to 3.3 V buck converter was used as an onboard converter for a pico-satellite. In [73], a buck topology was employed to regulate the voltage for CubeSat payloads (3.3 V and 5 V). Recently, a ripple-less buck converter was proposed to step down a 33 V satellite bus voltage to 1 V for LEO applications [74]. The converter uses an inverted AC current replica to cancel the ripple in the buck converter. Apart from the above-mentioned cases, the buck topology has also demonstrated its effectiveness for MPPT applications. For instance, a buck converter was used for MPPT (1500 W, 80 V to 28 V) in the Rosetta-Mars Express deep space mission [75]. A topology based on a buck converter was proposed by the authors of [76] for MPPT in nano-satellites. Without impacting the converter's efficiency, the current ripple was lowered by two coupled inductors at the load side. It also reduced the component count of the EPS. The converter was simulated using MATLAB, and the output confirmed its functionality under various source and load scenarios. In [77], two buck-derived converters, a redundant MPPT converter, and a redundant load-side converter were proposed for nano-satellites, comprising two half-bridge modules with a shared inductor and a fuse providing over-current protection. The redundant module is operative only under faulty conditions. Although the topology provides a fault diagnosis capability and improved reliability, its applicability for small satellites needs to be evaluated, considering the volume and weight restrictions of small satellites. A multi-stage EPS architecture for nano-satellites was proposed in [78], which used four buck converters for MPPT, load-side conversion, and battery charge regulation. Thus, in general, the conventional buck converter and its derivatives have demonstrated good performance with regard to PoL conversions and MPPT, especially for small satellites. While the conventional buck converter is not shown, the various buck-derived topologies of DC-DC converters discussed above are shown in Figure 9.

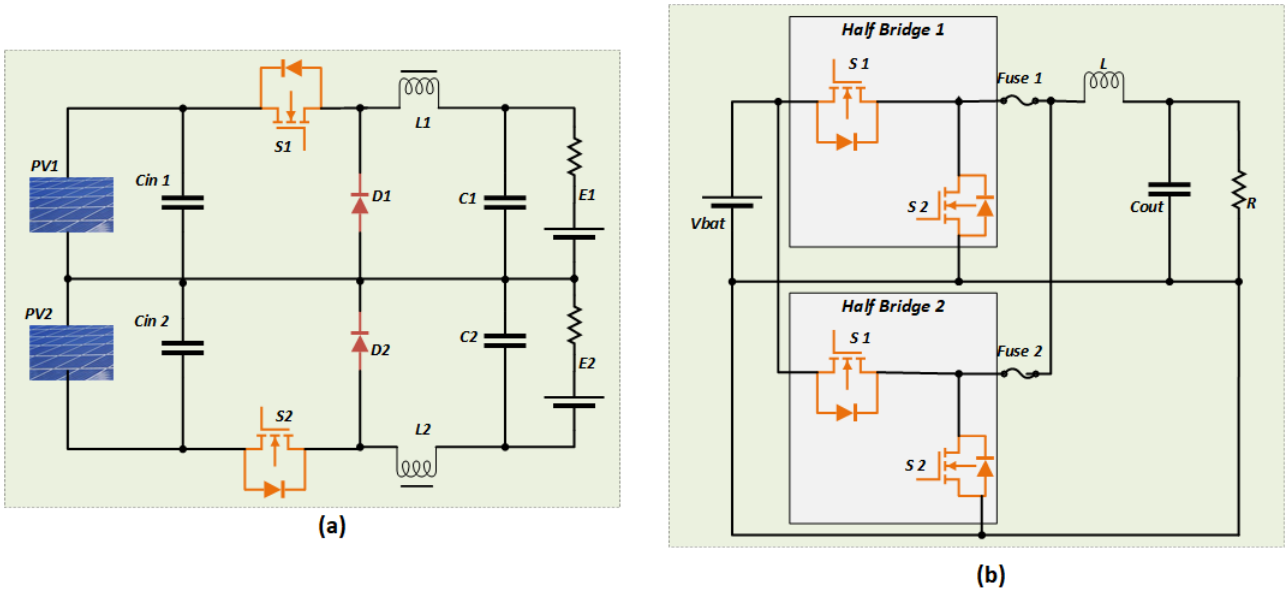

Figure 9. Buck-derived topologies (**a**) proposed in [76] and (**b**) proposed in [77].

3.1.2. Boost-Derived Topologies

A boost converter is predominantly used to implement MPPT on satellites. For instance, the Bepicolumbo mission to Mercury used a boost converter (12 kW, 100 V bus) for implementing MPPT [79]. Various boost-based topologies for satellite applications were compared and analyzed in [35] for MPPT applications, and based on the operating voltage range, power-handling capability, and output impedance of the solar array, the best topology was selected. Among these topologies, the conventional boost converter proved to be highly reliable due to its reduced device count. Nevertheless, the losses associated with the converter were high due to its reverse recovery diode. The switch-to-ground boost topology has a simple driving circuit and transfers energy directly from the input to the output. However, the topology has a high mass [35]. The topology was modified and proposed in [80] and is bidirectional with reduced mass and volume. The topology was specifically designed for high-power applications in LEO satellites. Another topology, the two-inductor boost topology proposed in [81], provides advantages like continuous input and output currents. However, the topology has two inductors and a poor dynamic response [35].

The ripple cancellation-based boost converter proposed in [82] has an additional branch to cancel ripple in the input current. However, the number of components in the converter increases due to the additional branch added [35]. The common-damping two-inductor boost converter was derived from the two-inductor boost converter by adding a damping network, showing improved bandwidth and a complicated power structure. However, the converter leads to increased losses in the magnetic components [35]. Interleaving boost converters reduce the component count, provide a good transient response, and significantly reduce the output current ripple [83]. A boost-based multiple-input, multiple-output interleaved topology was proposed in [84] for spacecraft applications. The converter implements MPPT and provides a fixed voltage at the output and battery control. Figure 10 shows the various boost-derived topologies of DC-DC converters.

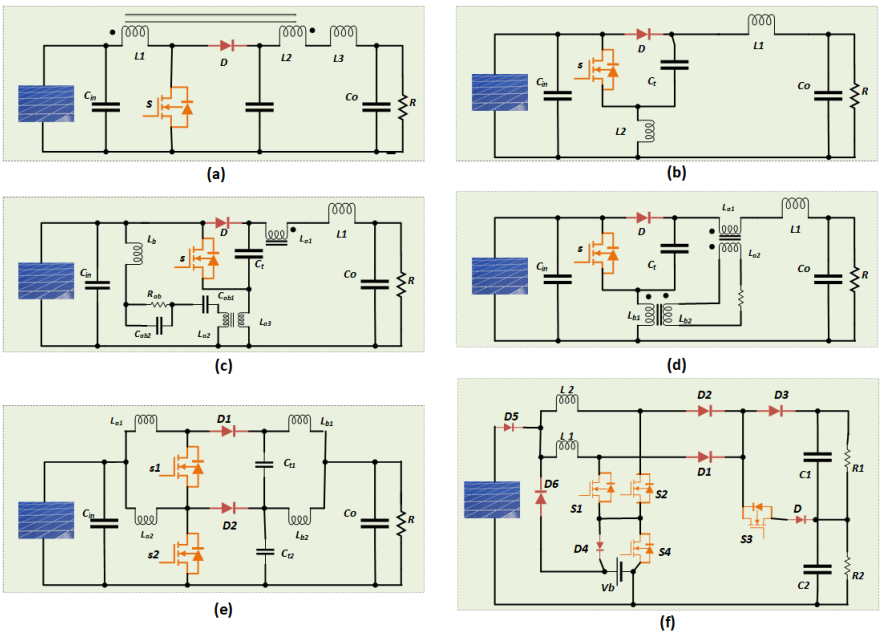

Figure 10. Boost-derived topologies: (**a**) boost converter with a near switch ground, (**b**) 2-inductor boost converter, (**c**) ripple cancellation-based boost converter, (**d**) common damping 2-inductor boost converter, (**e**) interleaved boost converter, (**f**) 2-input multiple-output interleaved boost converter.

Additionally, boost converters have also been proposed for battery discharge regulation in satellites, which regulate the bus voltage during eclipse periods. Ref. [85] proposed a family of 14 interleaved boost converters for BDRs in satellites. The converters demonstrated high efficiencies at output power ranging from 100 W to 1800 W. Due to the interleaved structure, all the converters showed good dynamic performance, no RHP zero effect, reduced filtering requirements, and low semiconductor device stresses. A similar application using a boost converter with an additional inductance was proposed in [86] for converting battery voltages between 55 V and 96 V to an average of 100 V output in satellites. An efficiency of about 97% was obtained with a reduced size. In general, boost converters have been mostly used for MPPT applications in small or large satellites, and their application as BDRs is also being studied.

3.1.3. Buck–Boost-Derived Topologies

Buck–boost-based converters have voltage step-up or step-down capabilities. The MPPT realization using a buck converter and a boost converter has the disadvantage that the efficiency decreases significantly as the difference between MPP voltage and bus voltage increases [44]. To overcome this, [44] proposed a buck–boost regulator (B2R) for application in regulated or unregulated bus systems for satellite EPSs. The topology demonstrated good performance and ensured that the bus voltage followed the maximum power-point PV voltage to maximize efficiency.

Later, in [87], this topology was modified to the buck–buck–boost regulator (B3R) for regulated bus systems, especially for LEO satellites. The topology was obtained by merging the B2R topology and two-inductor buck topologies. It performs two functions: a step-up function from the PV to the storage unit and a step-down function from the storage unit to the regulated bus. By sharing some passive components for the solar array and bus power regulation, the converter benefits in terms of mass and cost. Moreover, it can be made modular to improve redundancy. In [88], a four-switch buck–boost converter based on GaN and employing an RCC-MPPT controller for deep-space missions was proposed. Although the simulation results of the converter showed high efficiency and power density, experimental validations were not provided. Finally, in [89], an improved bidirectional Weinberg topology was proposed for battery charge/discharge regulation. The topology combines the Weinberg topology [90] and the buck topology, leading to high power density, efficiency, and a non-complex structure. In addition, it also provides bidirectional power flow capabilities and works in buck or boost modes.

Figure 11 shows the various buck–boost-derived topologies of DC-DC converters.

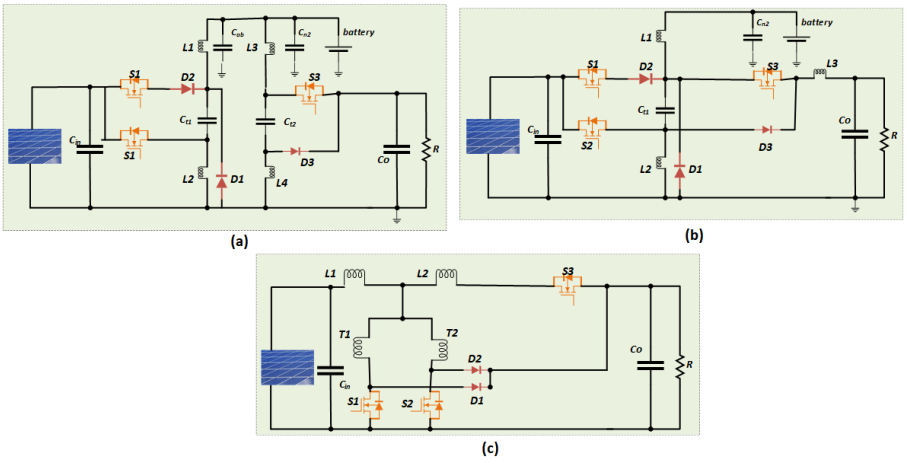

Figure 11. Buck–boost-derived topologies: (**a**) B2R converter, (**b**) B3R converter, (**c**) improved Weinberg topology.

3.1.4. Other Non-Isolated Topologies

In addition to the buck, boost, and buck–boost topologies, other topologies have been discussed in the literature for satellite applications. For instance, in [73], a SEPIC converter was used to implement MPPT for a CubeSat. In contrast to the conventional buck–boost converter, the SEPIC converter provides a positive polarity output and does not have the problem of floating switches during switching phases. Nevertheless, the converter's efficiency is very low under full irradiation conditions. Another study employed a SEPIC converter with a latching relay to implement MPPT in CubeSats [4]. The latching relay helps charge the battery directly from the solar array without MPPT under low-voltage conditions. The experimental results demonstrated the improved reliability of the converter. In [91], a one-switch constant power equalization charger using a multiple-stack buck–boost converter was proposed for the series connection of supercapacitors in satellites. The multiple-stack buck–boost converter can be realized using the SEPIC, Cuk, and Zeta converters. A 25 W prototype of the system using a SEPIC converter showed promising results. The literature does not provide other demonstrations of buck–boost converters, such as the Cuk and Zeta, for satellite applications. A comparison of the non-isolated topologies discussed above, in terms of the switching frequency, component count, type of satellite, and power, is provided in Table 1.

3.2. Isolated Topologies

This section discusses the various isolated DC-DC converters for satellite applications. Isolated converters are mainly required for secondary power distribution (as demonstrated in Figure 5e–g) in satellites to interface the satellite bus with a wide variety of payloads. The galvanic isolation between the input and output helps to attain effective power transfer with minimal noise and electromagnetic interference. It can be provided through a coupled inductor or using a transformer. The classification of various isolated DC-DC converters for satellites is shown in Figure 12.

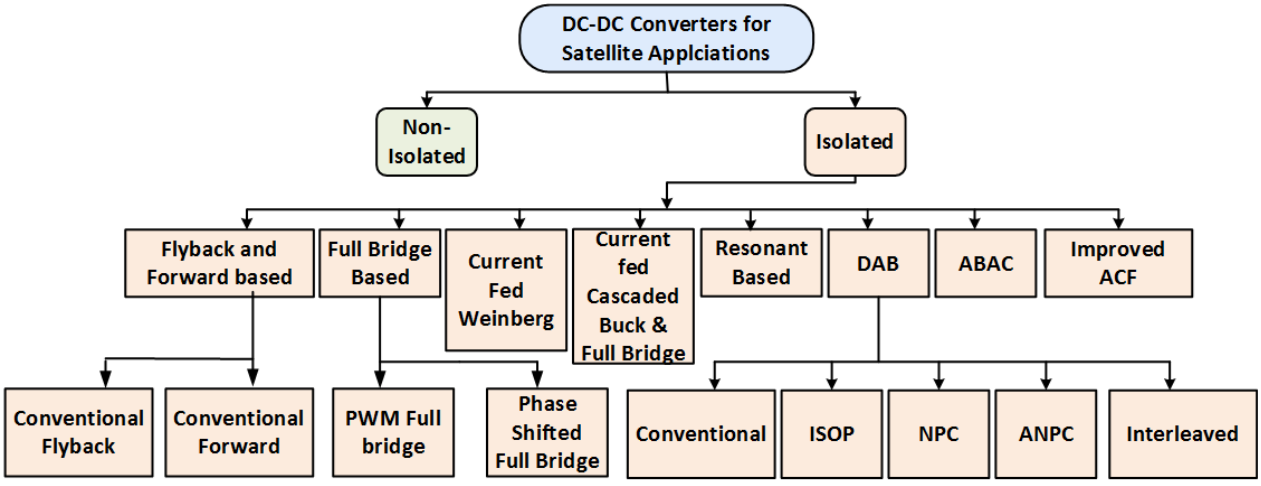

Figure 12. Classification of isolated DC-DC converters for satellite applications.

Table 1. Comparison of various non-isolated DC-DC converters.

Converter	References	Switching Frequency (kHz)	Component Count				Type of Satellite	Power (W)	Main Features
			S	D	L	C			
Conventional buck	[71–73]	-	1	1	1	1	Nano, pico, cube	Low	Good voltage regulation
Differentially connected buck [Figure 9a]	[36,76]	400	2	2	2	4	Nano-sat	30	Common mode noise rejection to reduce leakage current
Load-side redundant buck [Figure 9b]	[36,77]	-	4	0	1	1	Cube-sat	-	Redundant module for over-current protection
Switch-to-ground boost [Figure 10a]	[35,36]	130	1	1	3	3	Small sat	500	Simple driving circuits, direct energy transfer from input and output, high mass
	[80]	100	2	0	2	3	Small sat	5000	Low mass and volume
Two-inductor-based boost [Figure 10b]	[35,36,81]	130	1	1	2	2	Small sat	500	Continuous input and output currents, poor dynamic response.
Boost with ripple cancellation [Figure10c]	[35,36,82]	130	1	1	3	5	Small sat	500	Ripple cancellation, high component count
Common-damping 2-inductor boost [Figure 10d]	[35,36]	130	1	1	1	3	Small sat	500	High bandwidth, high loss in magnetic components
Interleaved boost [Figure 10e]	[35,36]	130	2	2	4	4	Small sat	500	Low output current ripple, good transient response, good transient response
Multi-output interleaved [Figure 10f]	[35,84]	100	4	7	2	2	-	500	
B2R converter [Figure 11a]	[35,44]	100	3	3	4	6	-	450	Good voltage regulation
B3R converter [Figure 11b]	[35,87]	-	3	3	3	4	-	-	Good voltage regulation and transient response.
Improved Weinberg converter [Figure 11c]	[35,89]	50	3	2	4	2	-	-	Simple structure, high efficiency, and power density

3.2.1. Flyback and Forward Converters

Flyback converters and forward converters are single-switch isolated DC-DC converters that are popular for low-power applications due to their simple design and low component count. A multiple-output converter based on a flyback converter was proposed in [92]. The topology provides advantages like good load regulation, line regulation, and high efficiency. Ref. [93] proposed an isolated multiple-output forward converter with magnetic feedback. The converter is reliable, as the magnetic feedback and controllers are not affected by the environmental conditions in space. However, topologies based on flyback or forward converters exhibit high semiconductor switching stresses and have low efficiency. Moreover, they exhibit low transformer utilization [94].

3.2.2. Full-Bridge Converter

Full-bridge converters are popular due to their features like good transformer core utilization, simple circuits, low-voltage switch stress, and good power-handling capacity [95]. Ref. [96] studied the full-bridge converter for high-power satellite applications. The converter operates over a wide output voltage range with good efficiency. Nonetheless, the output diodes' speed determines the switching frequency. Also, the converter is prone to shoot-through problems. A comparison of the phase-shifted full-bridge converter with the PWM full-bridge converter showed that the phase-shifted PWM has an inherent soft-switching capability and offers higher efficiency. However, it also faces similar problems with switching frequency and shoot-through. Nevertheless, its control strategy is more complex compared to the PWM full-bridge converter, making it a poor choice for high-power satellite applications. The circuit topology of a basic full-bridge converter is shown in Figure 13a.

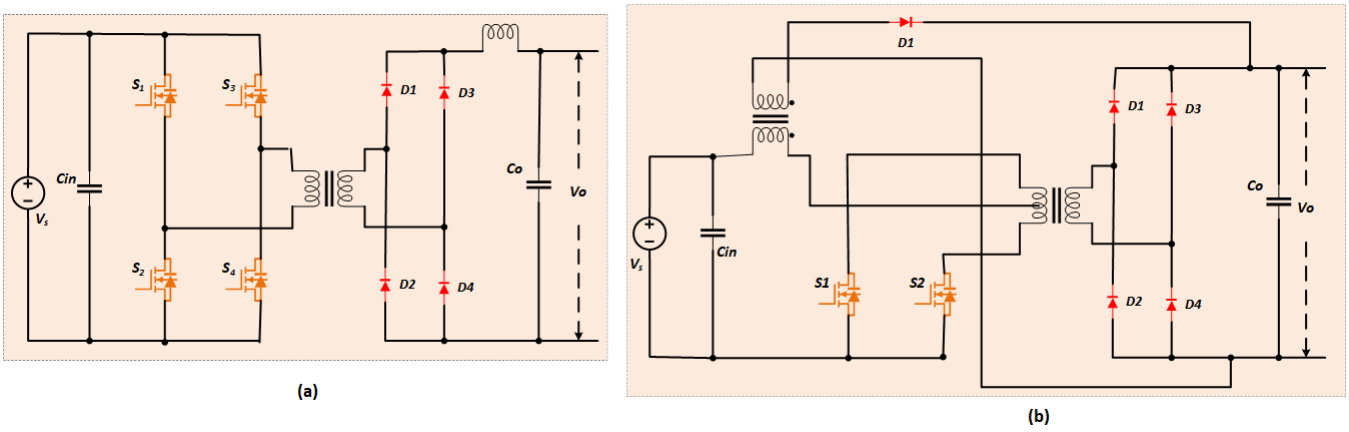

Figure 13. (**a**) Full-bridge converter. (**b**) Current-fed Weinberg converter.

3.2.3. Current-Fed Weinberg Converter

The benefits of using the current-fed Weinberg topology for satellite applications were investigated in [96,97]. Compared to the full-bridge converter, this converter is shoot-through tolerant, and the input voltage spans a broad range without compromising efficiency. However, its disadvantage lies in the high stresses on the semiconductor devices. The circuit topology is shown in Figure 13b.

3.2.4. Current-Fed Cascaded Buck and Full-Bridge Converter

A current-fed converter based on the cascaded buck and full-bridge topology was investigated in [96]. The converter is shoot-through tolerant and has a wide output voltage range. However, its high component count, limitation in operating frequency, and

lower efficiency due to additional switching stages are the disadvantages of this topology. Figure 14a shows the circuit topology of a current-fed cascaded buck and full-bridge converter.

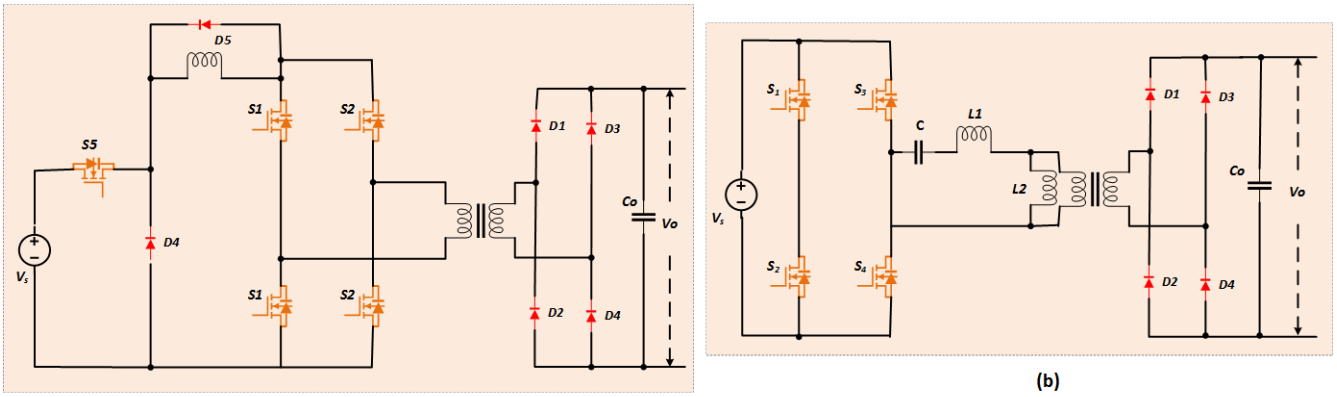

Figure 14. (**a**) Current-fed cascaded buck and full-bridge converter. (**b**) Resonant LLC converter.

3.2.5. Resonant Converters

Resonant converters, like isolated LLC and LCC resonant DC-DC converters, as well as series resonant converters that use resonant networks to achieve zero-voltage or zero-current switching, have been proposed for satellite applications [96,98]. In terms of efficiency, the resonant LLC converter is superior, and the LCC converter is superior in the input or output voltage range. In [99], a two-stage factorized power architecture was proposed for power distribution in satellites, in which the second stage adopts an interleaved LLC resonant converter. The converter has high efficiency and power density over a wide voltage range. Recently, a SiC-based T-type three-level LLC resonant converter was proposed in [100] and experimentally demonstrated for a 500 W, 48 V/11 A satellite application. A novel modulation scheme was used to achieve a wide output voltage range and high efficiency in the converter. Although resonant converters are highly efficient and have reduced mass, they require complex control circuitry [96]. Figure 14b shows the circuit of a basic resonant LLC converter.

3.2.6. Dual-Active Bridge Converter

The Dual-Active Bridge (DAB) topology has been widely accepted among researchers over the past couple of years for high-power density applications. It exhibits high performance and efficiency with inherent galvanic isolation and soft-switching capabilities. It is well-suited for handling high power and has a simple structure and high transformer utilization factor [95,101]. In a study by NASA [102], a bidirectional interleaved DAB converter was studied for satellite EPSs. A prototype of the converter (2 kW per module) using 650 V GaN semiconductors was developed and tested under cryogenic conditions. The study demonstrated the benefits of using the DAB converter for satellite EPSs. Several works have been proposed in the literature based on DAB converters for high-power applications in electric aircraft. As the study in [102] opened new possibilities for DAB converters for satellite applications and because the design limitations for electric aircraft and satellites are comparable (although not the same), these topologies are discussed in this review.

Ref. [103] performed the modeling, design, implementation, and performance evaluation of the DAB converter using SiC switches for aircraft electrical power networks. Ref. [104] compared the conventional DAB, Active Neutral Point Clamped (ANPC), Neutral Point Clamped (NPC), and Input-Series Output-Parallel (ISOP) converters using Wide-Band-Gap (WBG) devices for more electrical aircraft (MEA) applications.

Figure 15a–e show these DAB topologies. A comparison in terms of efficiency, heat management, power density, specific power, and EMC is shown in Figure 15f [104]. The figure illustrates the superiority of the ANPC type concerning efficiency, heat regulation, and power density. The ISOP and conventional DAB converters exhibit comparable results, with the conventional DAB showing higher efficiency. Although the NPC converter provides the best EMC performance along with the ANPC type, it shows poor performance in terms of the other three parameters. The design of a conventional DAB converter for space applications was discussed in [105].

Regarding the modulation strategy, single-phase-shift modulation is the most widely used method in DAB converters due to its simplicity [106,107]. Advanced modulation methods, like extended or dual-phase-shift modulation and triangular or trapezoidal current modulation, were proposed in [67,108]. Ref. [109] proposed an interleaved parallel DAB topology with a coupled inductor for MEA and compared the converter's performance with three modulation methods viz. single-phase shift, extended phase shift, and PWM plus single-phase shift. The topology is shown in Figure 15e. According to the study, single-phase shift combined with PWM can handle at least twice the power of a conventional DAB converter, while an extended phase shift can lower the current stress.

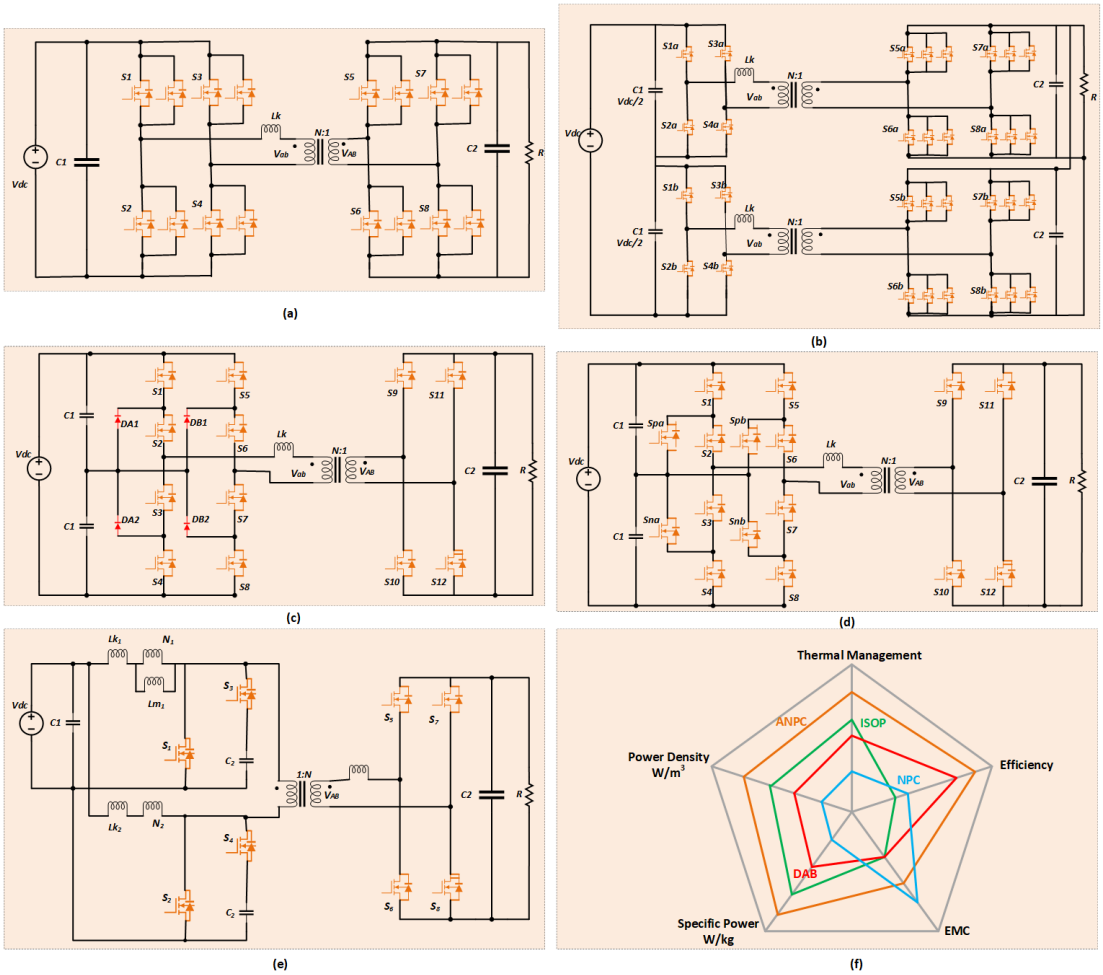

Figure 15. DAB converter topologies: (**a**) conventional, (**b**) ISOP type, (**c**) NPC type, (**d**) ANPC type, (**e**) parallel interleaved type. (**f**) Comparison of power density, thermal management, volume, efficiency, and EMI of various DAB converters.

3.2.7. Active-Bridge Active-Clamp Converter

Another topology of the DC-DC converter for aerospace applications with galvanic isolation is the Active-Bridge Active-Clamp (ABAC) topology [98] as shown in Figure 16a. Its operating behavior is similar to that of the DAB converter. However, it provides a current-fed LV stage. Ref. [67] compared various parameters of the ABAC converter with those of the DAB converter. A constant current on the DC side, due to interleaved inductors with reduced filter requirements on the LV side, makes the ABAC converter superior to the DAB converter. Nevertheless, a capacitor filter is required to control the ripple resulting from asymmetries in the topology and from harmonics in the load current. A comparison of the weight and volume of the ABAC and DAB converters was provided in [67], showing that in DAB converters, the weight is mainly contributed by capacitors, whereas in ABAC converters, a major part of their weight and volume is contributed by inductors. Nonetheless, the inductance values associated with ABAC converters are relatively low, which reduces the converter's weight and volume. This tendency becomes more evident at higher powers, making these converters a strong candidate for high-power applications. Thus, the ABAC converter is a suitable replacement for the DAB converter, without loss of efficiency and with improved power density.

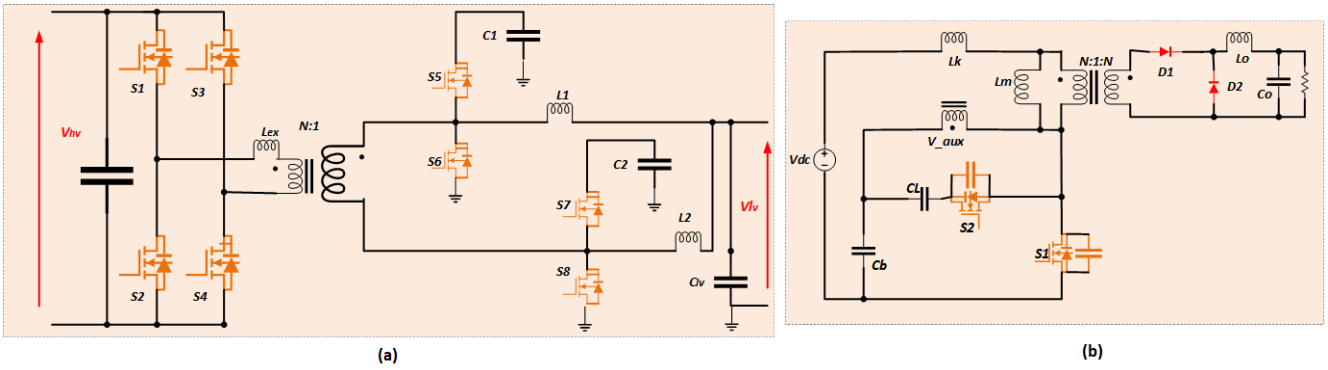

Figure 16. (**a**) Active-bridge active-clamp converter. (**b**) Improved active-clamp forward converter.

3.2.8. Active-Clamp Forward Converter

Ref. [110] proposed an improved active-clamp forward (ACF) converter to develop a reliable, lightweight, and EMI-compatible EPS for satellites. Although the ACF converter has a simple structure, fewer components, and clamping properties, its oscillating input current, high di/dt value, and voltage stress across the switches demand a larger filter size and make it a poor choice, especially for high-input-voltage applications. These problems were addressed with the improved ACF proposed in [110], which uses two series-connected switches to decrease semiconductor stresses. Moreover, during turn-off, a delay is provided to avoid the imbalance in switch voltage stress.

The experimental results also revealed a lower ripple in the current on the input side. Thus, the improved ACF topology is a strong contender for satellites that require high power density. Figure 16b shows the improved ACF topology proposed in [110]. A comparison of isolated DC-DC converters in terms of the switching frequency, component count, and power is shown in Table 2.

Table 2. Comparison of various isolated DC-DC converters.

Converter	References	Switching Frequency (kHz)	Component Count				Power (W)	Main Features
			S	D	L	C		
Full-bridge converter [Figure 13a]	[96]	50	4	4	1	2	1000	Wide output voltage, good efficiency, shoot-through problems.
Current-fed Weinberg converter [Figure 13b]	[96]	50	2	5	0	2	500	Shoot-through tolerant, high efficiency, wide output voltage, suitable for LV applications, HV stress across switches.
	[111]	150	2	3	1	1	1500	Fast dynamic response.
Current-fed cascaded buck and full-bridge converter [Figure 14a]	[96]	50	5	6	1	1	1000	Shoot-through tolerant, high component count, limitation in operating frequency, lower efficiency
Resonant LLC converter [Figure 14b]	[96]	>200	4	4	2	2	1000	High efficiency, lower weight, high switching frequency, complex control circuitry.
Conventional DAB [Figure 15a]	[104]	-	8	0	1	2	-	Soft switching, galvanic isolation, simple structure.
	[67]	100	8	0	1	2	8400	
ISOP-DAB [Figure 15b]	[104]	16	0	2	4		-	Low EMI noise, low efficiency.
NPC-DAB [Figure 15c]	[104]	-	12	4	1	3	-	Low volume and weight, low EMI noise, low efficiency.
ANPC-DAB [Figure 15d]	[104]	-	16	0	1	3	-	High efficiency, good heat management, high power density.
Parallel interleaved DAB [Figure 15e]	[104]	50	8	0	5	4	250	
ABAC converter [Figure 16a]	[67,98]	100	8	0	3	4	8400	High efficiency, high power density.
ACF [Figure 16b]	[110]	300	2	2	3	3	100	Reliable, lightweight, low EMI noise, high power density.

3.3. Integrated Topologies

This section reviews the various integrated multi-port converter topologies for application in satellites. In integrated multi-port topologies, switches and storage elements are shared during various operating modes, reducing component count and conversion stages. They are compact and have improved reliability compared to several independent converters performing the same task. A classification of integrated DC-DC topologies is provided in Figure 17a.

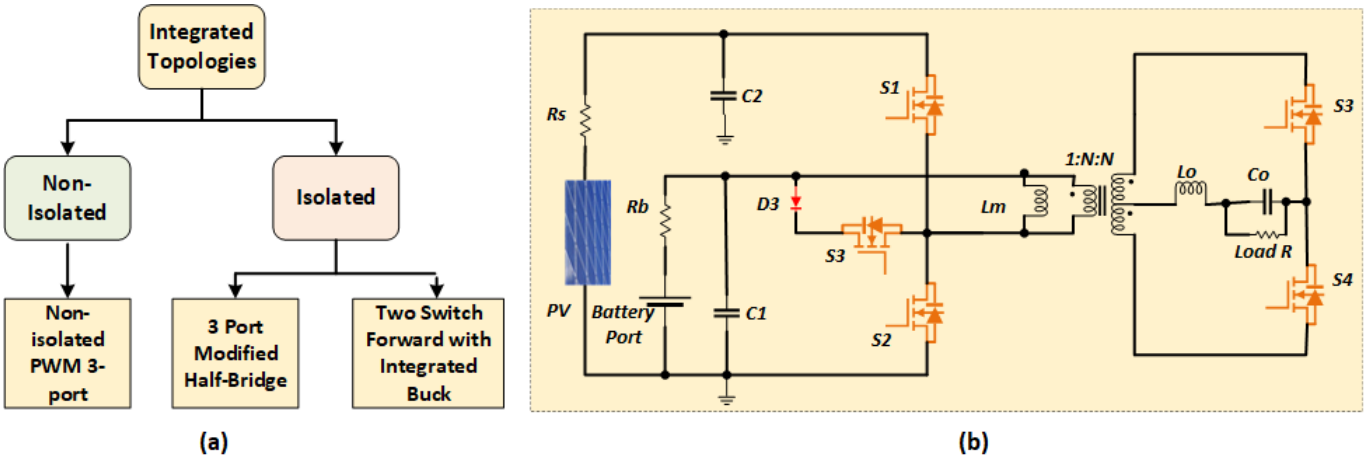

Figure 17. (**a**) Classification of integrated topologies of DC-DC converters for satellite applications. (**b**) Three-port modified half-bridge converter.

3.3.1. Three-Port Modified Half-Bridge Converter

Ref. [38] proposed a three-port DC-DC converter (TPC) with one input port from the solar array, one bidirectional port from the battery, and an isolated output port. The topology achieves zero-voltage switching for all semiconductors and reduces on-state losses by adopting synchronous rectification on the secondary side. A generalized method for modeling a three-port converter was also provided in the paper. However, the converter employs a complex control technique. Figure 17b shows the three-port modified half-bridge converter.

3.3.2. Non-Isolated PWM Three-Port Converter

In TPCs, the duty cycle during each pulse cycle is shared among many input ports. This effectively reduces the duty cycle of individual ports, leading to increased RMS currents and reduced efficiency [112,113]. Moreover, problems due to unshared grounds and the complexity of control circuits also exist [37]. To overcome such challenges, Ref. [114] proposed a novel non-isolated PWM TPC using a uni- and bidirectional PWM converter, as shown in Figure 18a. The converter is simple, avoids unshared ground issues, has higher effective duty cycles, and reduces inductor sizes. The size of passive elements in the converter decreased by about 19%, compared to the conventional non-isolated TPC.

3.3.3. Two-Switch Forward with Integrated Buck Converter

In [18], the heritage design properties of DC-DC converters for satellites were shown to align with the International Satellite Electronics Design Standards [115]. According to the study, the following design characteristics must be met by a DC-DC converter designed for satellite EPSs:

- Non-Leg Structure: The converter should have a conservative design in which a fault at a node should not interrupt the functioning of the entire system, thus ensuring an

extended life for the satellite. A non-leg structure was proposed in [115] as a potential solution in this context.

- PWM Controlled: To align with the strict EMI and EMC regulations in space and considering the variations in passive components in space, pulse-frequency modulation control is not recommended for DC-DC converters for satellites. Thus, PWM control is the proposed method of control [115].

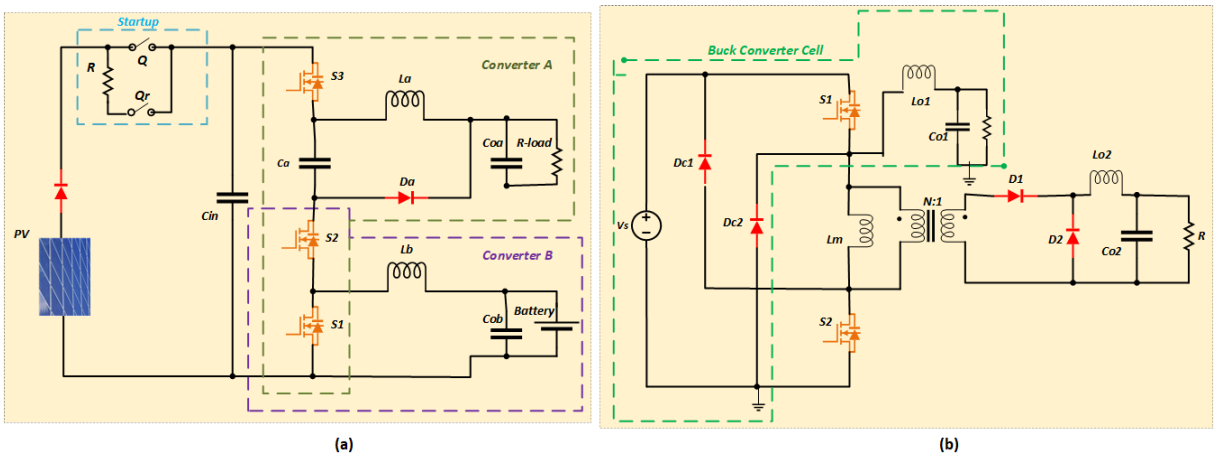

Figure 18. (**a**) Non-isolated PWM TPC. (**b**) Two-switch forward with integrated buck converter.

To create a DC-DC converter architecture that complies with the aforementioned requirements, the authors of [18] developed the topology shown in Figure 18b. A buck converter and a forward converter are combined, thus eliminating a diode and a switch. As a result, the topology's cost, mass, and volume decrease. Furthermore, ZVS is obtained for a few switches, increasing the efficiency of the converters. The above-mentioned integrated topologies are compared in terms of their switching frequency, power, and component count in Table 3.

Table 3. Comparison of various integrated DC-DC converters.

Converter	References	Switching Frequency (kHz)	Component Count				Power (W)	Isolated/Non-Isolated	Main Features
			S	D	L	C			
Three-port modified half-bridge converter [Figure 17b]	[38]	-	5	1	2	3	200	Isolated	Soft switching during turn-on, complex control technique.
Non-isolated PWM three-port converter [Figure 18a]	[37]	100	3	2	2	4	240	Non-isolated	Simple circuit, reduced size.
Two-switch forward with integrated buck converter [Figure 18b]	[18]	100	2	4	3	2	600	Isolated	Low mass and volume, ZVS switching, improved efficiency.

3.4. DC-DC Converters for Electric Propulsion

The PPU of the EP unit uses a highly efficient, isolated converter for voltage conversion. The topology selection depends on the type of satellite and the thruster. For small satellites, the pulsed plasma thruster (PPT) is a preferable choice [116–118]. It stores and discharges energy in the form of short pulses through a pair of electrodes. The energy storage function in PPTs is achieved using capacitor banks, and a DC-DC converter is used to charge and discharge the capacitor. The small satellite's input voltage is minimal, but the PPT thruster needs a very high DC output voltage. Therefore, to attain such high gain, a high-voltage, low-power DC-DC converter is needed. Moreover, the instantaneous release of energy from the capacitor into the thruster creates large reverse voltages, which may damage the sensitive electronic components. Thus, isolated DC-DC converters are the preferred

choice. In [117], a flyback converter was proposed, and the results were demonstrated for a 20W CubeSat, achieving an efficiency of 88%. To overcome the low efficiencies of the flyback converter, [116] proposed a boost–flyback converter operating in DCM and critical conduction mode for a similar application. In [118], a full-bridge LLC resonant topology was used for EP for micro- and nano-satellites. A 10 W prototype of the converter was developed to validate the performance.

For large satellites, the Hall-effect thruster and the gridded ion thruster are predominantly used. In [119], a 15 kW, 400 V discharge supply for the PPU of a Hall-effect thruster using SiC was proposed. The system uses two parallel full-bridge modules, each operating at 7.5 kW, 300 V nominal voltage. A 200 W prototype of the converter demonstrated an efficiency of around 92%. In [120], a resonant converter-based 4 kW discharge supply for a Hall-effect thruster was proposed. The converter demonstrated good performance over a broad spectrum of input and output conditions. A PPU for a 6 kW Hall-effect thruster with a wide output voltage range was proposed by JAXA in [121]. The output current and voltage ranges of the converter are 4 to 34 A and 175 to 800 V, respectively. The design is based on four 1.5 kW modules, which switch between series and parallel connections for multiple output connections. The modular structure significantly minimizes the thermal and mechanical design. An efficiency of 96% and a power density of 0.3 kW/kg were obtained. The control algorithm for the thruster was discussed in [122]. A forward converter-based heating power supply for a Hall-effect thruster was proposed in [123]. A 150 W experimental prototype of the system demonstrated an efficiency of 90%.

A 5 kW PPU for a 40 cm gridded ion thruster was proposed in [124]. The design was based on a phase-shift-modulated/PWM DAB converter, which showed high power density and efficiency. Ref. [125] proposed a combined dual modulation scheme for an all-electric propulsion system. The lower RMS or peak current under ZVS due to the combined dual modulation helps achieve high efficiency and good transient response throughout the whole operating range of the converter. Furthermore, it performs well against EMI noise as well. The control scheme was validated using a 1 kW–5 kW DAB converter [125].

A two-stage DC-DC converter comprising a four-switch interleaved buck–boost converter and an LLC resonant converter was proposed in [126] for high-power PPU in an ion propulsion system. The interleaving method used in the first stage reduced the magnitude of the magnetic components, and the soft-switched LLC resonant converter improved efficiency. Furthermore, using transformer leakage inductance as resonant inductance offered a high power density. A 1.2 kW prototype demonstrated good efficiency and power density. The first stage of the converter is shown in Figure 19, and a comparison of topologies for EP based on switching frequency, component count, and power is presented in Table 4.

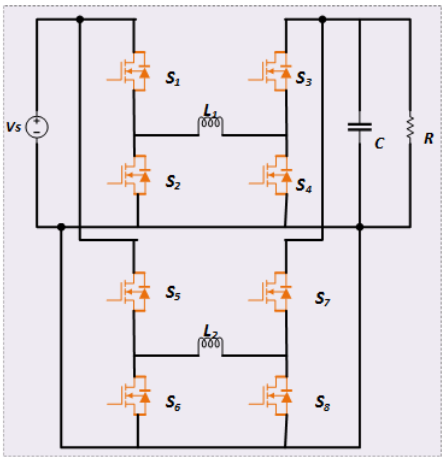

Figure 19. Four-switch interleaved buck–boost converter.

Table 4. Comparison of various DC-DC converters for EP in satellites.

Converter	References	Switching Frequency (kHz)	Component Count				Power (W)	Main Features
			S	D	L	C		
Flyback	[116,117]	-	1	1	1	1	20 W	Simple circuit, suitable for small satellites.
Resonant LLC	[118]	-	4	8	1	6	10 W	Simple circuit, suitable for small satellites.
Forward converter	[123]	100	1	1	1	1	150 W	Simple circuit, low component count.
Resonant LLC [Figure 14b]	[120]	>200	4	4	2	2	1 kW	High efficiency, lower weight, high switching frequency, complex control circuitry.
4 parallel converters	[122]	50	-	-	-	-	6 kW	High efficiency over wide output range, low component count, parallel or serial switching of converters to obtain multiple output conditions
DAB [Figure 15a]	[124,127]	-	8	0	1	2	5 kW	Soft switching, galvanic isolation, simple structure.
DAB with combined dual modulation [Figure 15a]	[125]	-	8	0	1	2	1–5 kW	Decreased EMI, a large output voltage range, high efficiency, and power density.
4-switch interleaved buck–boost + LLC resonant [Figure 19]	[126]	-	8	0	2	1	1.2 kW	Soft switching, low size of inductor, high power density, and efficiency.

4. Comparative Analysis of Various Topologies

This section provides a performance analysis and comparison of the various DC-DC converter topologies for satellite applications. The most important consideration for satellite applications is reliability, which must be weighed against other factors like converter cost, efficiency, and power density. Switching devices and their control circuits are considered the parts most prone to failure in a power converter. The lower the component count, the greater the reliability. Capacitors are also prone to failure, especially during high-temperature operations. Although they are troublesome and their reliability is uncertain, they are unavoidable. Space-grade components are used to improve performance, although at an increased cost [128]. Redundancy and modularity are two important means of improving reliability.

To improve the converter's power density, the switching frequency can be increased to minimize the size of the passive components while still meeting design specifications. Nevertheless, a larger switching frequency results in increased switching losses and has higher heat dissipation requirements [129]. This also leads to reduced efficiency. Therefore, a trade-off exists between power density, efficiency, and heat dissipation requirements in the converter [130]. Regarding efficiency, high-efficiency operation reduces fuel consumption and extends the satellite's life. Moreover, it results in lower heat dissipation requirements, lower costs, and improved reliability and power density. Semiconductor devices account for most of the losses in power converters, reducing efficiency, especially at high powers. Thus, in high-power satellite applications, parallel connection of several modules is adopted, so that each module carries only a fraction of the total power [104]. This helps improve the efficiency of the converter. Moreover, it also enhances performance by increasing the redundancy, ease of maintenance, scalability, and fault ride-through capabilities of the converter [131]. A schematic demonstration showing the above-mentioned dependencies of various performance parameters for satellite applications is provided in Figure 20. A comparison of isolated, non-isolated, and integrated topologies, as well as the topologies for EP, based on their reliability, redundancy, modularity, power density, and efficiency, is shown in Tables 5–8, respectively. The power density and efficiency values presented in the tables are obtained from the corresponding references, and reliability is classified as

low, medium, or high, based on the component count, redundancy, and modularity of the converter. Additionally, the topologies are classified based on application type and satellite type, as shown in Table 9.

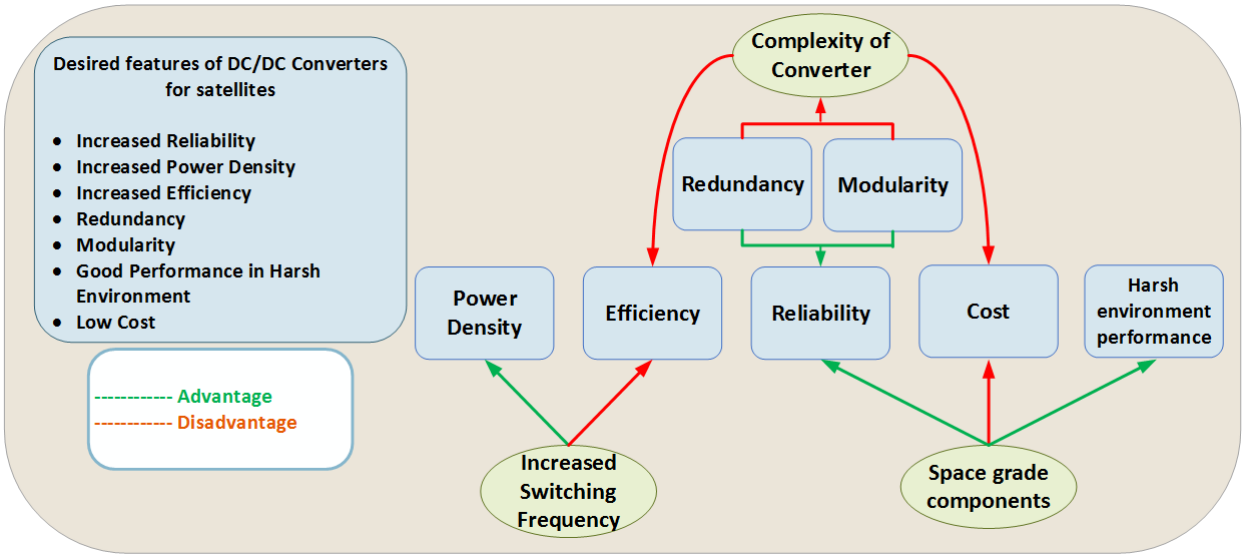

Figure 20. Various performance indicators of DC-DC converters for satellite applications.

Table 5. Comparison of various non-isolated DC-DC converters in terms of performance indicators.

Converter	References	Figure	Reliability	Redundancy	Modularity	Power Density	Efficiency
Differentially connected buck	[36,76]	Figure 9a	Medium	Yes	No	High	97
Load-side redundant buck	[36,77]	Figure 9b	High	Yes	No	-	-
Switch-to-ground buck	[35,36]	Figure 10a	High	No	No	-	96
Two-inductor-based boost	[35,36,81]	Figure 10b	High	No	No	-	>96
Boost with ripple cancellation	[35,36,82]	Figure 10c	Medium	No	No	High	>96
Common-damping 2-inductor boost	[35,36]	Figure 10d	High	No	No	-	>96
Interleaved boost	[35,36]	Figure 10e	High	Yes	yes	-	>96
Multi-output interleaved boost	[35,84]	Figure 10f	High	Yes	Yes	-	96
B2R Converter	[35,44]	Figure 11a	Medium	No	No	-	96
B3R Converter	[35,87]	Figure 11b	High	Yes	Yes	-	High
Improved Weinberg converter	[35,89]	Figure 11c	Medium	No	No	-	High

Table 6. Comparison of various isolated DC-DC converters in terms of performance indicators.

Converter	References	Figure	Reliability	Redundancy	Modularity	Power Density	Efficiency
Full-bridge converter	[96]	Figure 13a	Medium	No	No	Medium	95
Current-fed Weinberg converter	[96]	Figure 13b	High	No	No	Medium	95
Current-fed cascaded buck and full-bridge converter	[96]	Figure 14a	Medium	No	No	Medium	90–95
Resonant LLC converter	[96]	Figure 14b	Medium	No	No	Medium	95–98
Conventional DAB	[104]	Figure 15a	High	No	No	Medium	High
ISOP-DAB	[104]	Figure 15b	High	Yes	Yes	Medium	High
NPC-DAB	[104]	Figure 15c	Low	No	No	Low	Low
ANPC-DAB	[104]	Figure 15d	Low	No	No	High	High
Parallel interleaved DAB	[104]	Figure 15e	High	Yes	Yes	High	-
ABAC converter	[67,98]	Figure 16a	Low	Yes	Yes	High	High
ACF converter	[110]	Figure 16b	High	Yes	Yes	High	90–95

Table 7. Comparison of various integrated DC-DC converters in terms of performance indicators.

Converter	References	Figure	Reliability	Redundancy	Modularity	Power Density	Efficiency
Three-port modified half-bridge converter	[38]	Figure 17b	Low	No	No	Low	High
Non-isolated PWM three-port converter	[37]	Figure 18a	Medium	No	No	Medium	97.3
Two-switch forward with integrated buck converter	[18]	Figure 18b	High	No	No	High	95

Table 8. Comparison of various DC-DC converters in PPU for EP.

Converter	Ref.	Figure	Type of Thruster	Reliability	Redundancy	Modularity	Power Density	Efficiency
Resonant LLC	[120]	Figure 14b	Hall thruster	Medium	No	No	High	>95
4 parallel converters	[122]	-	Hall thruster	High	No	Yes	High	96.1
DAB	[124,127]	Figure 18	Ion thruster	Medium	No	No	High	High
DAB with combined dual modulation	[125]	Figure 18	-	High	No	No	High	-
4-switch interleaved buck–boost + LLC resonant	[126]	Figure 19	Ion thruster	High	No	Yes	High	High

Table 9. Comparison of the selected topologies based on their application in satellites and the type of satellite.

Application	Figure	Reference	Large	Small	Mini	Micro	Nano	Pico	Femto
MPPT	Figure 9a	[36,76]				✓	✓	✓	
	Figure 9b	[36,77]				✓	✓	✓	
	Figure 10a	[35,36]	✓	✓					
	Figure 10b	[35,36,81]	✓	✓					
	Figure 10c	[35,36,82]	✓	✓					
	Figure 10d	[35,36]	✓	✓					
	Figure 10e	[35,36]	✓	✓					
	Figure 10f	[35,84]	✓	✓					
	Figure 11a	[35,44]							
	Figure 11b	[35,87]							
Battery Regulator	Figure 10f	[35,84]	✓	✓					
	Figure 11b	[35,87]							
	Figure 11c	[35,89]							
Voltage Regulation	Figure 9a	[36,76]				✓	✓	✓	
	Figure 9b	[36,77]				✓	✓	✓	
	Figure 10a	[35,36]	✓	✓					
	Figure 10b	[35,36,81]	✓	✓					
	Figure 10c	[35,36,82]	✓	✓					
	Figure 10d	[35,36]	✓	✓					
	Figure 10e	[35,36]	✓	✓					
	Figure 10f	[35,84]	✓	✓					
	Figure 11a	[35,44]							
	Figure 11b	[35,87]							
	Figure 11c	[35,89]							
Multi-Port Conversion	Figure 17b	[38]		✓	✓	✓	✓	✓	✓
	Figure 18a	[37]		✓	✓	✓	✓	✓	✓
	Figure 18b	[18]		✓	✓	✓	✓	✓	✓
Electric Propulsion	Figure 14b	[96]	✓	✓					
	Figure 15a	[104]	✓	✓					
	Figure 19	[126]	✓	✓					
Power Distribution	Figure 13a	[96]	✓	✓					
	Figure 13b	[96]	✓	✓					
	Figure 14a	[96]	✓	✓					
	Figure 14b	[96]	✓	✓					
	Figure 15a	[104]	✓	✓					
	Figure 15b	[104]	✓	✓					
	Figure 15c	[104]	✓	✓					
	Figure 15d	[104]	✓	✓					
	Figure 15e	[104]	✓	✓					
	Figure 16a	[67,98]	✓	✓					
	Figure 16b	[110]		✓	✓				

5. Future Directions

When discussing the future challenges for power electronics in satellite applications, the main expected change is the increase in power [132]. This adds additional design constraints for power converters like the need for better heat dissipation equipment, availability of components that can tolerate high power, reduction of EMI, and reduction in weight and volume of magnetic components. The increase in power could be tackled by increasing the voltage of the main bus, hence limiting the current flow and reducing the cable weight [133]. Moreover, increased voltage levels demand a better selection of

converter topology, power device packaging, and magnetic components. In summary, although increasing the bus voltage level is an effective solution with regard to increased power levels in satellites, several hurdles need to be overcome to achieve the same [130].

5.1. Wide-Band-Gap Devices

New technologies like WBG devices (SiC and GaN) provide better performance compared to Si technology [134–137]. Recent research on WBG devices has demonstrated their superior efficiency and power density compared to Si-based devices [138,139]. However, the capabilities of WBG devices cannot be fully exploited by simple replacement. System- and component-level refinements need to be performed. With the integration of WBG, switching frequencies above hundreds of kilohertz are theoretically allowed. This can help reduce the value of the inductors and hence the dimensions of the converter. Nonetheless, increasing the switching frequency poses various challenges, such as increased switching losses, parasitic effects, and heat management, which should be carefully studied. Additionally, the reliability of such devices for application in space needs to be studied in detail, especially their performance under radiation regarding single-event effect (SEE) and single-event burnout (SEB) [140]. Heat management at high power levels, which affects the efficient operation of a power converter, is another open area of research in the future [141].

5.2. Deep Space Missions

The unbounded, limitless area of space that extends beyond the Moon to Mars and throughout our solar system is known as deep space. Comprehending the planets, moons, and minor bodies within our solar system facilitates our exploration of the past, the diversity of our own and other planetary systems, and our understanding of our origins. Thus, deep space missions are expected to show remarkable progress in the near future. Spacecraft need to be resilient to the harsh environmental conditions in space, and strong propulsion and communication systems are required for spacecraft to be able to accomplish this. For such missions, electric propulsion is thought to be a crucial and innovative technology. Furthermore, interest in using small satellites for exploring deep space is growing. The BepiColombo, GOCE, and SMART-1 missions by ESA are a few examples. NASA is also exploring electric propulsion for deep space missions. For instance, the Lunar Gateway's power and propulsion component is expected to showcase cutting-edge, high-power solar electric propulsion. Figure 21 shows a few present and future deep space missions along with their power levels [142,143]. It is evident that the power requirements for deep space missions show an increasing trend. This increase in power demands intensive research on novel DC-DC converters that can work reliably and efficiently in such radiation-hardened environments.

5.3. Solar Power Satellites

Space-based solar power (SBSP) is a method in which solar energy in space is harvested for utilization on Earth. SBSP necessitates wireless power transmission via microwaves, laser, or by reflecting sunlight directly. It is expected to change the future of electricity generation and distribution by producing electricity in an efficient and pollution-free manner. A wireless energy grid may involve beaming power from Earth to space and back. The spacecraft may also be located in different orbits, such as LEO or GEO. Although the technology has enormous potential, it is still in the conceptual stage. Several obstacles must be overcome, resulting in a new area of research for future scientists and engineers [144–146].

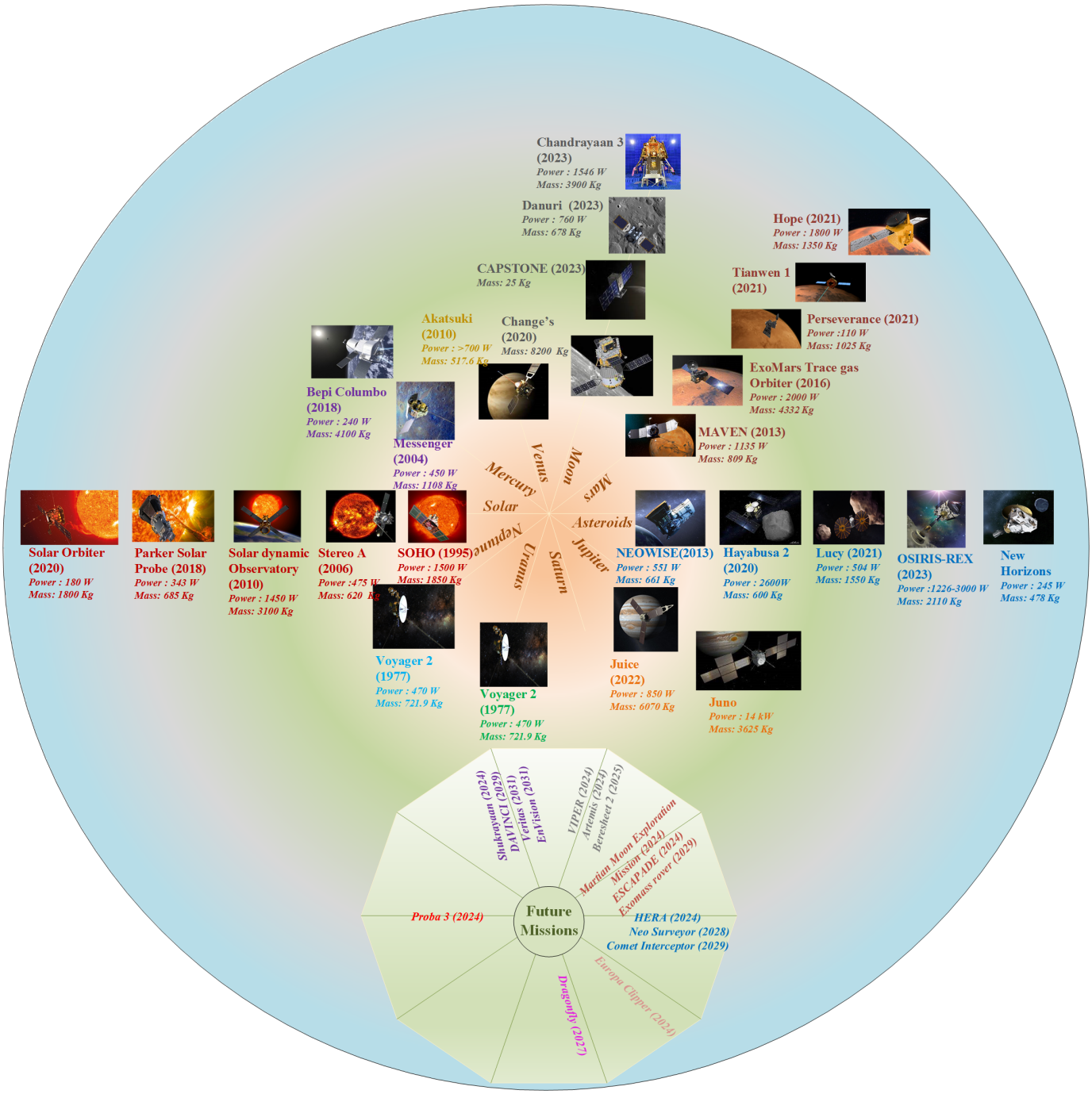

Figure 21. Various deep space missions, along with their power and mass.

5.4. Wireless Power Transfer for Satellite Power Distribution

In dusty and harsh environments, where physical connectors may deteriorate, Wireless Power Transfer (WPT) is considered acceptable, especially for small satellites. Although the efficiency of WPT systems is relatively low, with sufficient research and development, it can be a potential method for power transfer in space applications. WPT is especially helpful in improving the reliability and robustness of regulation and transmission of power [10,147,148]. This opens up new avenues of research in the design and development of highly efficient DC-DC converters for wireless power transfer in space. A summary of a few identified research gaps in various space applications is provided in Table 10.

Table 10. Research gaps in various space applications.

Area	Research Gaps
Design and Development of DC-DC Converters	• Improve fault-tolerant capability without increasing size. • Avoid common mode current for fail-safe operation. • Improve power density. • Reduce ripple content of output current to improve battery health. • Improve reliability by avoiding single-element failure. • Solve unshared ground issues in multi-port converters. • Increase power levels for converters (>100 kW). • Increase output voltage range (>300 V). • Increase high-voltage conversion ratio. • Improve efficiency and power density. • Design modular converters. • Improve the design of input and output EMI filters.
Adoption of Solar EP/Nuclear EP	• Improve the specific impulse and durability of high-thrust systems. • Improve the efficiency and reliability of low-thrust systems. • Increase power levels (>100 kW). • Increase understanding of the reliability and lifetime of propulsion systems at higher power levels. • Reduce specific mass.
Deep Space Exploration	• Develop electronic components capable of withstanding high radiation and temperatures in deep space. • Develop high-power propulsion systems. • Develop new materials and technologies to enhance the efficiency and durability of solar panels in deep space.
Electronic Components for Space Applications	• Develop higher-rating space-grade SiC and GaN semiconductors • Design PCB layouts and packaging techniques with low parasitics for WBG devices. • Design gate drivers for switches. • Study the reliability of WBG devices under cryogenic and radiation-hardened environments. • Develop EMI mitigation methods. • Develop high-current/high-energy-density capacitors. • Develop low-loss magnetic materials that can withstand high temperatures.
Solar-Based Power Satellites	• Develop low-cost solar cells with a long lifetime. • Investigate Perovskite solar cells. • Develop large-scale microwave/laser-based wireless energy transfer methods. • Develop kilometer-scale space solar power plants.

6. Conclusions

DC-DC converters are critical for generating, transmitting, and storing power in satellites. This paper classifies the applications of DC-DC converters in satellites and provides a state-of-the-art review of isolated and non-isolated DC-DC converters for a range of satellite applications. The topologies are compared based on practical parameters like modularity, efficiency, reliability, redundancy, and power density. Electric propulsion is a promising future technology owing to its better fuel efficiency compared to chemical propulsion. Thus, various sources and DC-DC converters for electric propulsion are compared and contrasted. The research gaps pertaining to a variety of current and prospective satellite application domains, such as space-based solar power and wireless power transmission for satellite power distribution, are also highlighted in this paper.

Author Contributions: Conceptualization, R.R and A.M.M.; methodology, R.R.; formal analysis, R.R.; investigation, R.R.; resources, R.R.; data curation, R.R.; writing—original draft preparation, R.R. and A.M.M.; writing—review and editing, R.R. and A.M.M.; supervision, A.M.M.; project administration, A.M.M.; funding acquisition, A.M.M. All authors have read and agreed to the published version of the manuscript.

Funding: This publication was supported by Qatar University through the Graduate Assistantship program. The statements made herein are the sole responsibility of the authors.

Data Availability Statement: No new data were created or analyzed in this study.

Conflicts of Interest: The authors declare no conflicts of interest.

Abbreviations

The following abbreviations are used in this manuscript:

ABAC	Active-Bridge Active-Clamp
ACF	Active-Clamp Forward
ANPC	Active Neutral Point Clamped
B2R	Buck–Boost Regulator
B3R	Buck–Buck–Boost Regulator
BCR	Battery Charge Regulator
BDR	Battery Discharge Regulator
DAB	Dual Active Bridge
DET	Direct Energy Transfer
EMI	Electromagnetic Interference
EP	Electric Propulsion
EPS	Electrical Power System
GEO	Geosynchronous Earth Orbit
IC	Incremental Conductance
ISOP	Input-Series Output-Parallel
LEO	Low Earth Orbit
MEA	More Electric Aircraft
MEO	Medium Earth Orbit
MPPT	Maximum Power-Point Tracking
NPC	Neutral Point Clamped
P&0	Perturb and Observe
PCDU	Power Conditioning and Distribution Unit
PPT	Pulsed Plasma Thruster
PPU	Power Processing Unit
RCC	Ripple Correlation Control
RTG	Radioisotope Thermoelectric Generator
S3R	Sequential Switching Shunt Regulator
S4R	Sequential Series Shunt Regulator
SBSP	Space-Based Solar Power
SEE	Single-Event Effect
SEB	Single-Event Burnout
TPC	Three-Port Converter
WBG	Wide Band Gap
WPT	Wireless Power Transfer

References

1. Murugan, P.; Agrawal, Y. Small satellites applications, classification and technologies. *Int. J. Sci. Res. (IJSR)* **2020**, *9*, 1682–1687. [CrossRef]
2. Wu, J.; Deng, L.; Praks, J.; Anger, M.; Oleynik, P.; Hajdas, W.; Wang, J.D.; Zhang, S.Y.; Zhou, B.; Zeng, L.; et al. CORBES: Radiation belt survey with international small satellite constellation. *Adv. Space Res.* **2024**. [CrossRef]
3. Sweeting, M.N. Modern small satellites-changing the economics of space. *Proc. IEEE* **2018**, *106*, 343–361. [CrossRef]
4. Chen, Y.K.; Lai, Y.C.; Lu, W.C.; Lin, A. Design and implementation of high reliability electrical power system for 2U NutSat. *IEEE Trans. Aerosp. Electron. Syst.* **2020**, *57*, 614–622. [CrossRef]
5. Barnwell, N.; Ritz, T.; Parry, S.; Clark, M.; Serra, P.; Conklin, J.W. The Miniature Optical Communication Transceiver—A Compact, Power-Efficient Lasercom System for Deep Space Nanosatellites. *Aerospace* **2018**, *6*, 2. [CrossRef]
6. Casado, P.; Torres, C.; Blanes, J.M.; Garrigós, A.; Marroquí, D. Implementation of a 6U CubeSat Electrical Power System Digital Twin. *Aerospace* **2024**, *11*, 688. [CrossRef]
7. Qu, Z.; Zhang, G.; Cao, H.; Xie, J. LEO satellite constellation for Internet of Things. *IEEE Access* **2017**, *5*, 18391–18401. [CrossRef]

8. Asher, J.; Acarregui, O.; Wang, J. Numerical Simulation of Ionic Electrospray Contamination for Small Satellite Formation Flight. *IEEE Trans. Plasma Sci.* **2023**, *51*, 2508–2514. [CrossRef]
9. Curzi, G.; Modenini, D.; Tortora, P. Large constellations of small satellites: A survey of near future challenges and missions. *Aerospace* **2020**, *7*, 133. [CrossRef]
10. State of the Art Small Spacecraft Technology Report. Available online: https://www.nasa.gov/smallsat-institute/sst-soa/ (accessed on 25 September 2024).
11. The Lunar Atmosphere and Dust Environment Explorer(LADEE). Available online: https://science.nasa.gov/mission/ladee/ (accessed on 25 September 2024).
12. Cyclone Global Navigation Satellite System. Available online: https://www.nasa.gov/cygnss (accessed on 25 September 2024).
13. AeroCube 7-OCSD-A (AeroCube 7-Optical Communication and Sensor Demonstration-A). Available online: https://www.eoportal.org/satellite-missions/aerocube-ocsd (accessed on 25 September 2024).
14. ALBA ORBITAL. Available online: http://www.albaorbital.com/unicorn-2 (accessed on 25 September 2024).
15. Barato, F.; Toson, E.; Milza, F.; Pavarin, D. Investigation of different strategies for access to space of small satellites on a defined LEO orbit. *Acta Astronaut.* **2024**, *222*, 11–28. [CrossRef]
16. Ocean Surface Topography from Space. Available online: https://sealevel.jpl.nasa.gov/missions/jason-1/summary/ (accessed on 25 September 2024).
17. Satellite Batteries—For CubeSats, Nanosats, and Other form Factors. Available online: https://blog.satsearch.co/2021-06-23-satellite-batteries-for-cubesats-nanosats-and-other-form-factors (accessed on 25 September 2024).
18. Park, J.E.; Han, J.K.; Choi, S.H.; Moon, G.W. Two-switch forward converter with an integrated buck converter for high bus voltage in satellites. *IEEE Trans. Power Electron.* **2022**, *38*, 2041–2051. [CrossRef]
19. Gonzalez-Llorente, J.; Lidtke, A.A.; Hatanaka, K.; Kawauchi, R.; Okuyama, K.I. Solar module integrated converters as power generator in small spacecrafts: Design and verification approach. *Aerospace* **2019**, *6*, 61. [CrossRef]
20. Lim, T.M.; Cramer, A.M.; Lumpp, J.E.; Rawashdeh, S.A. A modular electrical power system architecture for small spacecraft. *IEEE Trans. Aerosp. Electron. Syst.* **2018**, *54*, 1832–1849. [CrossRef]
21. Cao, M.; Zhang, T.; Yu, B.; Liu, Y. A method for interval prediction of satellite battery state of health based on sample entropy. *IEEE Access* **2019**, *7*, 141549–141561. [CrossRef]
22. Tan, B.; Tseng, K. Intelligent and reliable power supply system for small satellites. In Proceedings of the 25th International Telecommunications Energy Conference, Yokohama, Japan, 23–23 October 2003; INTELEC'03; IEEE: Piscataway, NJ, USA, 2003; pp. 249–255.
23. Edpuganti, A.; Khadkikar, V.; El Moursi, M.S.; Zeineldin, H.; Al-Sayari, N.; Al Hosani, K. A comprehensive review on CubeSat electrical power system architectures. *IEEE Trans. Power Electron.* **2021**, *37*, 3161–3177. [CrossRef]
24. Park, J.E.; Han, J.K.; Park, K.B.; Lee, B.H.; Moon, G.W. A new direct charging control for electrical power systems in low Earth orbit satellites. *IEEE Trans. Aerosp. Electron. Syst.* **2022**, *59*, 2566–2578. [CrossRef]
25. O'Reilly, D.; Herdrich, G.; Kavanagh, D.F. Electric propulsion methods for small satellites: A review. *Aerospace* **2021**, *8*, 22. [CrossRef]
26. Sun, L.; Zhao, Z.; Huang, H.; Zhao, X. A thrust inversion method for small satellite electric propulsion based on a momentum wheel. *Acta Astronaut.* **2024**, *219*, 982–995. [CrossRef]
27. Sahoo, S.; Zhao, X.; Kyprianidis, K. A review of concepts, benefits, and challenges for future electrical propulsion-based aircraft. *Aerospace* **2020**, *7*, 44. [CrossRef]
28. Pedrini, D.; Misuri, T.; Paganucci, F.; Andrenucci, M. Development of hollow cathodes for space electric propulsion at sitael. *Aerospace* **2017**, *4*, 26. [CrossRef]
29. Gagne, K.R.; McDevitt, M.R.; Hitt, D.L. A Dual Mode Propulsion System for Small Satellite Applications. *Aerospace* **2018**, *5*, 52. [CrossRef]
30. Fu, M.; Zhang, D.; Li, T. New electrical power supply system for all-electric propulsion spacecraft. *IEEE Trans. Aerosp. Electron. Syst.* **2017**, *53*, 2157–2166. [CrossRef]
31. Caverly, R.J.; Di Cairano, S.; Weiss, A. Electric satellite station keeping, attitude control, and momentum management by MPC. *IEEE Trans. Control Syst. Technol.* **2020**, *29*, 1475–1489. [CrossRef]
32. Saha, A.; Ghassemi, M. Optimal design of high-power density medium-voltage direct current bipolar power cables for lunar power transmission. *Aerospace* **2024**, *11*, 685. [CrossRef]
33. Spacecraft Bus Voltage Selection 2015 Space Power Workshop 12–14 May 2015. Available online: https://ntrs.nasa.gov/api/citations/20150019744/downloads/20150019744.pdf (accessed on 28 October 2024).
34. He, Y.; Perreault, D.J. Lightweight high-voltage power converters for electroaerodynamic propulsion. *IEEE J. Emerg. Sel. Top. Ind. Electron.* **2021**, *2*, 453–463. [CrossRef]
35. Garcia, O.; Alou, P.; Oliver, J.A.; Diaz, D.; Meneses, D.; Cobos, J.A.; Soto, A.; Lapena, E.; Rancano, J. Comparison of boost-based MPPT topologies for space applications. *IEEE Trans. Aerosp. Electron. Syst.* **2013**, *49*, 1091–1107. [CrossRef]

36. Yaqoob, M.; Lashab, A.; Vasquez, J.C.; Guerrero, J.M.; Orchard, M.E.; Bintoudi, A.D. A comprehensive review on small satellite microgrids. *IEEE Trans. Power Electron.* **2022**, *37*, 12741–12762. [CrossRef]
37. Nagata, H.; Uno, M. Nonisolated PWM three-port converter realizing reduced circuit volume for satellite electrical power systems. *IEEE Trans. Aerosp. Electron. Syst.* **2020**, *56*, 3394–3408. [CrossRef]
38. Qian, Z.; Abdel-Rahman, O.; Al-Atrash, H.; Batarseh, I. Modeling and control of three-port DC/DC converter interface for satellite applications. *IEEE Trans. Power Electron.* **2009**, *25*, 637–649. [CrossRef]
39. Hussein, B.; Massoud, A.M.; Khattab, T. Optimized Load-Scheduling Algorithm for CubeSat's Electric Power System Management Considering Communication Link. *IEEE Trans. Aerosp. Electron. Syst.* **2023**, *59*, 7455–7468. [CrossRef]
40. National Aeronautics and Space Administration. *Small Spacecraft Technology State of the Art (TP-2015-216648)*; NASA Technical Publication: Moffett Field, CA, USA, 2015.
41. Hussein, B.; Massoud, A.M.; Khattab, T. Centralized, distributed, and module-integrated electric power system schemes in cubesats: Performance assessment. *IEEE Access* **2022**, *10*, 55396–55407. [CrossRef]
42. Edpuganti, A.; Khadkikar, V.; El Moursi, M.S.; Zeineldin, H. A novel multiport converter interface for solar panels of cubesat. *IEEE Trans. Power Electron.* **2021**, *37*, 629–643. [CrossRef]
43. Edpuganti, A.; Khadkikar, V.; Zeineldin, H.; El Moursi, M.S.; Al Hosani, M. Comparison of peak power tracking based electric power system architectures for CubeSats. *IEEE Trans. Ind. Appl.* **2021**, *57*, 2758–2768. [CrossRef]
44. Mourra, O.; Fernandez, A.; Tonicello, F. Buck boost regulator (B 2 R) for spacecraft solar array power conversion. In Proceedings of the 2010 Twenty-Fifth Annual IEEE Applied Power Electronics Conference and Exposition (APEC), Palm Springs, CA, USA, 21–25 February 2010; pp. 1313–1319.
45. Mostacciuolo, E.; Iannelli, L.; Sagnelli, S.; Vasca, F.; Luisi, R.; Stanzione, V. Modeling and power management of a LEO small satellite electrical power system. In Proceedings of the 2018 European Control Conference (ECC), San Antonio, TX, USA, 4–8 March 2018; pp. 2738–2743.
46. Kompella, M.; Kaarthik, R.S.; Priyadarshnam, H.; Simha, H. Parallel operation of battery chargers in small satellite electrical power systems. In Proceedings of the 2019 IEEE 16th India Council International Conference (INDICON), Rajkot, India, 13–15 December 2019; pp. 1–4.
47. Stevanovic, B.; Salinas López, G.; Alou Cervera, P.; Oliver Ramírez, J.A.; Vasic, M.; Cobos Márquez, J.A. Low power distribution module for space applications: Analysis and comparison of different architectures and dc/dc topologies. In Proceedings of the Presentation at Congress or Conference, Madrid, Spain, 23–24 March 2017.
48. Skup, K.R.; Grudziński, P.; Orleański, P.; Nowosielski, W. A digital controller for satellite medium power DC/DC converters. In Proceedings of the 2013 18th International Conference on Methods & Models in Automation & Robotics (MMAR), Miedzyzdroje, Poland, 26–29 August 2013; pp. 566–571.
49. Orts, C.; Garrigós, A.; Marroquí, D.; Franke, A. Sequential Switching Shunt Regulation Using DC Transformers for Solar Array Power Processing in High Voltage Satellites. *IEEE Trans. Aerosp. Electron. Syst.* **2024**, *60*, 421–429. [CrossRef]
50. Padial, P.M. Secondary Power Distribution in Satellites. Available online: https://www.doeeet.com/content/eee-components/draft-secondary-power-distribution-in-satellites (accessed on 25 September 2024).
51. Hosny, I.; Safwat, I.M.; Mokhtar, A.; Elewa, A. Sequential Switching Shunt Regulator S3R and Maximum Power Point Tracking MPPT for a 3U CubeSat. In Proceedings of the 2024 14th International Conference on Electrical Engineering (ICEENG), Cairo, Egypt, 21–23 March 2024; pp. 31–35.
52. Schirone, L.; Ferrara, M.; Granello, P.; Paris, C.; Pellitteri, F. Power bus management techniques for space missions in low earth orbit. *Energies* **2021**, *14*, 7932. [CrossRef]
53. Osullivan, D.; Weinberg, G. The sequential switching shunt regulator S3R. In Proceedings of the 3rd ESTEC Spacecraft Power Conditioning Seminar, Noordwijk, The Netherlands, 21–23 September 1977.
54. Blanes, J.M.; Carrasco, J.A.; Garrigós, A.; Marroquí, D.; Torres, C. Sequential switching shunt regulator parallel power processing control for high capacitance solar arrays. *Energies* **2021**, *14*, 429. [CrossRef]
55. Capel, A.; Perol, P. Comparative performance evaluation between the S4R and the S3R regulated bus topologies. In Proceedings of the 2001 IEEE 32nd Annual Power Electronics Specialists Conference (IEEE Cat. No. 01CH37230), Vancouver, BC, Canada, 17–22 June 2001; Volume 4, pp. 1963–1969. [CrossRef]
56. Eddine, K.K.D.; Lina, W.; Abderrahmane, S.; Messaoud, B.; de Oliveira Nogueira, P.H.; Boualem, K.M. Comprehensive Analysis and Design of Electrical Power Systems for Nanosatellite Platforms: A Focus on Robust MPPT Control Using Sliding Mode Control Method. *Int. J. Energy Res.* **2024**, *2024*, 4879696. [CrossRef]
57. Li, P.; Zhang, J.; Xu, R.; Zhou, J.; Gao, Z. Integration of MPPT algorithms with spacecraft applications: Review, classification and future development outlook. *Energy* **2024**, *308*, 132927. [CrossRef]
58. Mazouffre, S. Electric propulsion for satellites and spacecraft: Established technologies and novel approaches. *Plasma Sources Sci. Technol.* **2016**, *25*, 033002. [CrossRef]
59. Dale, E.; Jorns, B.; Gallimore, A. Future directions for electric propulsion research. *Aerospace* **2020**, *7*, 120. [CrossRef]

60. Potrivitu, G.C.; Sun, Y.; Rohaizat, M.W.A.b.; Cherkun, O.; Xu, L.; Huang, S.; Xu, S. A review of low-power electric propulsion research at the Space Propulsion Centre Singapore. *Aerospace* **2020**, *7*, 67. [CrossRef]
61. Yin, S.; Xin, X.; Wang, R.; Dong, M.; Lin, J.; Gu, Y.; Li, H. A 1-MHz GaN-Based *LCLC* Resonant Step-Up Converter With Air-Core Transformer for Satellite Electric Propulsion Application. *IEEE Trans. Ind. Electron.* **2021**, *69*, 11035–11045. [CrossRef]
62. Alnaqbi, S.; Darfilal, D.; Swei, S.S.M. Propulsion Technologies for CubeSats. *Aerospace* **2024**, *11*, 502. [CrossRef]
63. Davis, J.P.; Mayberry, J.P.; Penn, J.P. Cost Reductions and Fuel Efficiency: High-Power Solar Electric Propulsion in Space. In *Game Changer*; Technical Report; Aerospace Corporation: El Segundo, CA, USA, 2021. Available online: https://aerospace.org/sites/default/files/2018-11/Davis-Mayberry_HPSEP_11212018.pdf (accessed on 15 January 2025).
64. Space Nuclear Propulsion. Available online: https://www.nasa.gov/tdm/space-nuclear-propulsion/ (accessed on 28 October 2024).
65. Lev, D.; Myers, R.M.; Lemmer, K.M.; Kolbeck, J.; Koizumi, H.; Polzin, K. The technological and commercial expansion of electric propulsion. *Acta Astronaut.* **2019**, *159*, 213–227. [CrossRef]
66. Available online: https://www.satnow.com/community/what-is-a-power-processing-unit-ppu-for-thrusters (accessed on 28 October 2024).
67. Tarisciotti, L.; Costabeber, A.; Chen, L.; Walker, A.; Galea, M. Current-fed isolated DC/DC converter for future aerospace microgrids. *IEEE Trans. Ind. Appl.* **2018**, *55*, 2823–2832. [CrossRef]
68. Patnaik, B.; Kumar, S.; Gawre, S. Recent advances in converters and storage technologies for more electric aircrafts: A review. *IEEE J. Miniat. Air Space Syst.* **2022**, *3*, 78–87. [CrossRef]
69. Solsona, J.A.; Gomez Jorge, S.; Busada, C.A. Modeling and nonlinear control of DC–DC converters for microgrid applications. *Sustainability* **2022**, *14*, 16889. [CrossRef]
70. Yao, K.; Ye, M.; Xu, M.; Lee, F.C. Tapped-inductor buck converter for high-step-down DC-DC conversion. *IEEE Trans. Power Electron.* **2005**, *20*, 775–780. [CrossRef]
71. Houari, B.; Aissa, B.; Lakhdar, L.; Yazid, B.E. DC/DC buck Converter Prototype for Educational Nanosatellite Power Sub-System. In Proceedings of the 2023 International Conference on Advances in Electronics, Control and Communication Systems (ICAECCS), Blida, Algeria, 6–7 March 2023; pp. 1–6. [CrossRef]
72. Kulkarni, S.; Bangade, S.; Khadse, M.; Waghulde, D.; Aher, P.; Gaikwad, K.; Thakurdesai, S. Design and optimization of the on board DC/DC converters of Swayam satellite. In Proceedings of the 2014 IEEE International Conference on Power Electronics, Drives and Energy Systems (PEDES), Mumbai, India, 16–19 December 2014; pp. 1–6. [CrossRef]
73. Darbali-Zamora, R.; Cobo-Yepes, N.; Salazar-Duque, J.E.; Ortiz-Rivera, E.I.; Rincon-Charris, A.A. Buck converter and SEPIC based electronic power supply design with MPPT and voltage regulation for small satellite applications. In Proceedings of the 2017 IEEE 44th Photovoltaic Specialist Conference (PVSC), Washington, DC, USA, 25–30 June 2017; pp. 2963–2968.
74. Kao, Y.H.; Wu, J.L.; Liao, C.C.; Chang, H.H.; Huang, W.C.; Tsai, H.Y.; Guo, R.B.; Chen, K.H.; Zeng, K.L.; Lin, Y.H.; et al. A 33V to 1V Ripple-Less Buck Converter With the Inverted AC Current Replica Circuit and Sub-0.5 Application. *IEEE Solid-State Circuits Lett.* **2024**, *7*, 183–186. [CrossRef]
75. Jensen, H.; Laursen, J. Power conditioning unit for Rosetta/Mars express. In Proceedings of the Space Power, Porto, Portugal, 6–10 May 2002; Volume 502, p. 249.
76. Faujdar, J.; Gautam, D.K.; Verma, V. A new converter for common mode noise reduction for EPS of a nano satellite. In Proceedings of the 2020 IEEE First International Conference on Smart Technologies for Power, Energy and Control (STPEC), Nagpur, India, 25–26 September 2020; pp. 1–6.
77. Edpuganti, A.; Khadkikar, V.; Elmoursi, M.S.; Zeineldin, H.; Al Hosani, M. A novel EPS architecture for 1U/2U CubeSats with enhanced fault-tolerant capability. In Proceedings of the 2020 IEEE Industry Applications Society Annual Meeting, Detroit, MI, USA, 10–16 October 2020; pp. 1–6.
78. Chiu, S.Y.; Kim, K.A. System analysis and design for multiconverter electrical power systems in nanosatellites. *IEEE J. Miniat. Air Space Syst.* **2022**, *4*, 41–53. [CrossRef]
79. Hansen, M.M. Power conditioning unit for bepicolombo transfer module. In Proceedings of the 8th European Space Power Conference, Constance, Germany, 14–19 September 2008; Volume 661, p. 84.
80. Sanchis, E.; Maset, E.; Ferreres, A.; Ejea, J.B.; Esteve, V.; Jordan, J.; Calvente, J.; Garrigos, A.; Blanes, J.M. Bidirectional high-efficiency nonisolated step-up battery regulator. *IEEE Trans. Aerosp. Electron. Syst.* **2011**, *47*, 2230–2239. [CrossRef]
81. White, J.; Muldoon, W. Two-inductor boost and buck converters. In Proceedings of the 1987 IEEE Power Electronics Specialists Conference, Blacksburg, VA, USA, 21–26 June 1987; pp. 387–392.
82. Martinelli, R.; Ashley, C. Coupled inductor boost converter with input and output ripple cancellation. In Proceedings of the APEC'91: Sixth Annual Applied Power Electronics Conference and Exhibition, Dallas, TX, USA, 10–15 March 1991; pp. 567–572.
83. Hwu, K.I.; Yau, Y.T. An interleaved AC–DC converter based on current tracking. *IEEE Trans. Ind. Electron.* **2008**, *56*, 1456–1463. [CrossRef]

84. Gorji, J.G.; Abbaszadeh, K.; Bagheroskouei, F. A new two-input and multi-output interleaved DC_DC boost converter for satellites power system. In Proceedings of the 2019 10th International Power Electronics, Drive Systems and Technologies Conference (PEDSTC), Shiraz, Iran, 12–14 February 2019; pp. 236–241.
85. Zhu, H.; Zhang, D.; Liu, X.; Zhang, M.; Zhang, B. A Family of Interleaved Boost Converters for Battery Discharging in Space Applications. *IEEE Trans. Power Electron.* **2023**, *38*, 1887–1900. [CrossRef]
86. Geist, A.V.; Sidorov, A.V.; Korobkov, D.V.; Volkov, A.G. DC/DC Boost Converter with Additional Inductance for the Space Power Supply System. In Proceedings of the 2018 19th International Conference of Young Specialists on Micro/Nanotechnologies and Electron Devices (EDM), Erlagol, Russia, 29 June–3 July 2018; pp. 6403–6408. [CrossRef]
87. Mourra, O.; Fernandez, A.; Tonicello, F.; Landstroem, S. Multiple port DC DC converter for spacecraft power conditioning unit. In Proceedings of the 2012 Twenty-Seventh Annual IEEE Applied Power Electronics Conference and Exposition (APEC), Orlando, FL, USA, 5–9 February 2012; pp. 1278–1285.
88. Mahmud, S.; Collings, W.; Kini, R.; Javaid, A.; Khanna, R.; Barchowsky, A.; Loveland, J.; Amirahmadi, A.; Stell, C.; Zapien, X. A GaN-Based Four-Switch Buck-Boost Converter Using Ripple Correlation Control for Maximum Power Point Tracking in Dynamic Deep Space Environments. 2020. Available online: https://digitalcommons.usu.edu/smallsat/2020/all2020/163/ (accessed on 15 January 2025).
89. Qunhai, H.; Jingyuan, Y.; Lixin, W.; Tongzhen, W. Research on a new bidirectional DC-DC topology for space applications. In Proceedings of the 2017 12th IEEE Conference on Industrial Electronics and Applications (ICIEA), Siem Reap, Cambodia, 18–20 June 2017; pp. 1686–1690.
90. Weinberg, S.; Lopez, A. A bidirectional BDR/BCR for satellite applications. In Proceedings of the Fifth European Space Power Conference (ESPC), Tarragona, Spain, 21–25 September 1998; Volume 416, p. 27.
91. Uno, M.; Tanaka, K. Single-switch constant-power equalization charger based on multi-stacked buck-boost converters for series-connected supercapacitors in satellite power systems. In Proceedings of the 2011 IEEE Ninth International Conference on Power Electronics and Drive Systems, Singapore, 5–8 December 2011; pp. 1158–1165. [CrossRef]
92. Deepa, K.; Deepti, T.; Kumar, V. New multi-output switching converter with low drop out post regulator. In Proceedings of the 2013 International Conference on Emerging Trends in Communication, Control, Signal Processing and Computing Applications (C2SPCA), Bangalore, India, 10–11 October 2013; pp. 1–6.
93. Rampelli, P.K.; Deekshit, R.; Reddy, D.S.; Singh, B.K.; Chippalkatti, V.; Kanthimathinathan, T. Multiple-output magnetic feedback forward converter with discrete PWM for space application. In Proceedings of the 2012 IEEE International Conference on Power Electronics, Drives and Energy Systems (PEDES), Bengaluru, India, 16–19 December 2012; pp. 1–6.
94. ElMenshawy, M.; Massoud, A. Medium-voltage dc-dc converter topologies for electric bus fast charging stations: State-of-the-art review. *Energies* **2022**, *15*, 5487. [CrossRef]
95. Swaminathan, N.; Cao, Y. An overview of high-conversion high-voltage DC–DC converters for electrified aviation power distribution system. *IEEE Trans. Transp. Electrif.* **2020**, *6*, 1740–1754. [CrossRef]
96. Boomer, K. Investigation into High Power Converter Topologies. In Proceedings of the NASA Engineering and Safety Center (NESC) Electrical Power Technical Discipline Team (TDT) Meeting, Cleveland, OH, USA, 28 September 2021.
97. Tong, Q.; Zhang, H.; Zhang, D. Research on a High Power Density DC/DC Converter Based on Weinberg Topology. In Proceedings of the 2018 2nd IEEE Advanced Information Management, Communicates,Electronic and Automation Control Conference (IMCEC), Xi'an, China, 25–27 May 2018; pp. 2346–2350. [CrossRef]
98. Tarisciotti, L.; Costabeber, A.; Linglin, C.; Walker, A.; Galea, M. Evaluation of isolated DC/DC converter topologies for future HVDC aerospace microgrids. In Proceedings of the 2017 IEEE Energy Conversion Congress and Exposition (ECCE), Cincinnati, OH, USA, 1–5 October 2017; pp. 2238–2245.
99. Wang, L.; Zhang, D.; Yang, Y.; Li, H. Two-Stage Factorized Power Architecture DC–DC Converter for Spacecraft Secondary Power Supply System. *IEEE J. Emerg. Sel. Top. Power Electron.* **2022**, *10*, 5392–5413. [CrossRef]
100. Ma, W.; Li, H. A High Step-Down SiC-Based T-Type LLC Resonant Converter for Spacecraft Power Processing Unit. *Aerospace* **2024**, *11*, 396. [CrossRef]
101. Das, D.; Basu, K. Optimal design of a dual-active-bridge DC–DC converter. *IEEE Trans. Ind. Electron.* **2020**, *68*, 12034–12045. [CrossRef]
102. Bidirectional Dual Active Bridge Power Converter for Spacecraft Power Systems. Available online: https://techport.nasa.gov/projects/90266 (accessed on 28 October 2024).
103. Naayagi, R.; Forsyth, A.J.; Shuttleworth, R. High-power bidirectional DC–DC converter for aerospace applications. *IEEE Trans. Power Electron.* **2012**, *27*, 4366–4379. [CrossRef]
104. Keshmiri, N.; Hassan, M.I.; Rodriguez, R.; Emadi, A. Comparison of isolated bidirectional DC/DC converters using WBG devices for more electric aircraft. *IEEE Open J. Ind. Electron. Soc.* **2021**, *2*, 184–198. [CrossRef]

105. Pradhan, R.; Hassan, M.I.; Wang, Z.; Yuan, J.; Pietrini, G.; Suntharalingam, P.; Cruz, M.F.; Emadi, A. Design of a 20 kW Bidirectional Dual Active Bridge Converter for Aerospace Applications. In Proceedings of the 2023 IEEE Applied Power Electronics Conference and Exposition (APEC), Orlando, FL, USA, 19–23 March 2023; pp. 1024–1030.
106. Zhang, J.; Tang, Y.; Hu, W.; Zhang, Z.; Li, J.; Chen, Z. Minimum current stress operation of dual active half-bridge converter using triple phase shift control for renewable energy applications. *Energy Rep.* **2022**, *8*, 547–553. [CrossRef]
107. Xiao, Y.; Guan, Y.; Qin, L. Proposed asymmetric phase shift modulation strategy to improve zero-voltage-switch range and transmission power range for dual active bridge converter. *Energy Rep.* **2023**, *9*, 762–770. [CrossRef]
108. Naayagi, R.; Forsyth, A.; Shuttleworth, R. Performance analysis of extended phase-shift control of DAB DC-DC converter for aerospace energy storage system. In Proceedings of the 2015 IEEE 11th International Conference on Power Electronics and Drive Systems, Sydney, Australia, 9–12 June 2015; pp. 514–517.
109. Jiang, C.; Liu, H. A novel interleaved parallel bidirectional dual-active-bridge DC–DC converter with coupled inductor for more-electric aircraft. *IEEE Trans. Ind. Electron.* **2020**, *68*, 1759–1768. [CrossRef]
110. Lee, N.; Lee, J.Y.; Cheon, Y.J.; Han, S.K.; Moon, G.W. A high-power-density converter with a continuous input current waveform for satellite power applications. *IEEE Trans. Ind. Electron.* **2019**, *67*, 1024–1035. [CrossRef]
111. Weijun, L.; Yaujun, L. Small-signal modeling and analysis of the Weinberg converter for high-power satellites bus application. *Chin. J. Electron.* **2009**, *18*, 171–176.
112. Nahavandi, A.; Hagh, M.T.; Sharifian, M.B.B.; Danyali, S. A nonisolated multiinput multioutput DC–DC boost converter for electric vehicle applications. *IEEE Trans. Power Electron.* **2014**, *30*, 1818–1835. [CrossRef]
113. Uno, M.; Sugiyama, K. Switched capacitor converter based multiport converter integrating bidirectional PWM and series-resonant converters for standalone photovoltaic systems. *IEEE Trans. Power Electron.* **2018**, *34*, 1394–1406. [CrossRef]
114. Nagata, H.; Uno, M. Multi-port converter integrating two PWM converters for multi-power-source systems. In Proceedings of the 2017 IEEE 3rd International Future Energy Electronics Conference and ECCE Asia (IFEEC 2017-ECCE Asia), Kaohsiung, Taiwan, 4–7 June 2017; pp. 1833–1838.
115. Space Engineering Standard, ECSS-E-ST-20C. Available online: https://ecss.nl/standard/ecss-e-st-20c-electrical-and-electronic/ (accessed on 25 September 2024).
116. O'Reilly, D.; Herdrich, G.; Schäfer, F.; Montag, C.; Worden, S.P.; Meaney, P.; Kavanagh, D.F. A coaxial pulsed plasma thruster model with efficient flyback converter approaches for small satellites. *Aerospace* **2023**, *10*, 540. [CrossRef]
117. O'Reilly, D.; Kavanagh, D.F. Efficient Flyback Converter Design for Pulsed Plasma Thrusters with Applications in Cubesats. In Proceedings of the 2023 IEEE 2nd Industrial Electronics Society Annual On-Line Conference (ONCON), Virtual, 8–10 December 2023; pp. 1–6.
118. Singh, A.K.; Das, P.; Panda, S. High voltage high frequency resonant DC-DC converter for electric propulsion for micro and nanosatellites. In Proceedings of the 2014 IEEE 36th International Telecommunications Energy Conference (INTELEC), Vancouver, UK, 28 September–2 October 2014; pp. 1–5.
119. Piñero, L.R.; Scheidegger, R.J.; Aulsio, M.V.; Birchenough, A.G. High input voltage discharge supply for high power Hall thrusters using silicon carbide devices. In Proceedings of the International Electric Propulsion Conference (IEPC2013), Washington, DC, USA, 6–10 October 2014; Number NASA/TM-2014-216607.
120. Pinero, L.; Bowers, G. Multi-Kilowatt Power Module for High Power Hall Thrusters. In Proceedings of the 40th AIAA/ASME/SAE/ASEE Joint Propulsion Conference and Exhibit, Fort Lauderdale, FL, USA, 11–14 July 2004; p. 3973.
121. Matsunaga, Y.; Takahashi, T.; Watanabe, H.; Goto, D.; Cho, S.; Kusawake, H.; Kurokawa, F.; Kajiwara, K.; Funaki, I. Wide-output range power processing unit for 6-kW hall thruster. *IEEE Trans. Aerosp. Electron. Syst.* **2021**, *58*, 1609–1620. [CrossRef]
122. Matsunaga, Y.; Watanabe, H.; Cho, S.; Funaki, I.; Kusawake, H.; Kajiwara, K.; Kurokawa, F.; Takahashi, T. Control algorithm for a 6 kW hall thruster. *J. Electr. Propuls.* **2022**, *1*, 29. [CrossRef]
123. Zhou, J.; Zhu, Z.; Dong, B.; Wang, X.; Wang, Z.; Liu, T. Design of Heating Power Supply for Power Processing Unit of Hall Thruster. In Proceedings of the 2024 3rd International Conference on Energy and Electrical Power Systems (ICEEPS), Guangzhou, China, 14–16 July 2024; pp. 904–910.
124. Piñero, L.R.; Bond, T.; Okada, D.; Pyter, J.; Wiseman, S. Design of a modular 5-kw power processing unit for the next-generation 40-cm ion engine. In Proceedings of the 27th International Electric Propulsion Conference, Indianapolis, IN, USA, 7–10 July 2002; Number NASA/TM-2002-211359.
125. R, K.; N, L.N.; G, S. Combined Dual modulation Scheme (CDMS) for high power converters in Spacecraft All Electric Propulsion Systems (AEPS). In Proceedings of the 2022 IEEE International Conference on Power Electronics, Drives and Energy Systems (PEDES), Jaipur, India, 14–17 December 202; pp. 1–6. [CrossRef]
126. Huang, X.; Lan, J.; Chen, N.; Fang, T.; Ruan, X.; He, X. A novel two-stage DC/DC converter applied to power processing unit for astronautical ion propulsion system. In Proceedings of the 2019 IEEE International Conference on Industrial Technology (ICIT), Melbourne, Australia, 13–15 February 2019; pp. 343–348.

127. Youssef, T.; Löher, T.; Azzopardi, S. Embedded Power GaN Components inside a PCB for space applications. In Proceedings of the 2022 International Conference on Electronics Packaging (ICEP), Sapporo, Japan, 11–14 May 2022; pp. 11–12.
128. Ravyts, S.; Van De Sande, W.; Vecchia, M.D.; Broeck, G.V.d.; Duraij, M.; Martinez, W.; Daenen, M.; Driesen, J. Practical considerations for designing reliable DC/DC converters, applied to a BIPV case. *Energies* **2020**, *13*, 834. [CrossRef]
129. Sayed, K.; Almutairi, A.; Albagami, N.; Alrumayh, O.; Abo-Khalil, A.G.; Saleeb, H. A review of DC-AC converters for electric vehicle applications. *Energies* **2022**, *15*, 1241. [CrossRef]
130. Dorn-Gomba, L.; Ramoul, J.; Reimers, J.; Emadi, A. Power electronic converters in electric aircraft: Current status, challenges, and emerging technologies. *IEEE Trans. Transp. Electrif.* **2020**, *6*, 1648–1664. [CrossRef]
131. ElMenshawy, M.; Massoud, A. Modular isolated dc-dc converters for ultra-fast ev chargers: A generalized modeling and control approach. *Energies* **2020**, *13*, 2540. [CrossRef]
132. Chin, K.B.; Brandon, E.J.; Bugga, R.V.; Smart, M.C.; Jones, S.C.; Krause, F.C.; West, W.C.; Bolotin, G.G. Energy storage technologies for small satellite applications. *Proc. IEEE* **2018**, *106*, 419–428. [CrossRef]
133. Kerslake, T.W. Effect of voltage level on power system design for solar electric propulsion missions. *J. Sol. Energy Eng.* **2004**, *126*, 936–944. [CrossRef]
134. Phillips, A.; Cook, T.; West, B.; Grainger, B.M. Gallium nitride efficacy for high-reliability forward converters in spacecraft. *IEEE J. Emerg. Sel. Top. Power Electron.* **2022**, *10*, 5357–5370. [CrossRef]
135. Islam, R.; Rafin, S.S.H.; Mohammed, O.A. Comprehensive review of power electronic converters in electric vehicle applications. *Forecasting* **2022**, *5*, 22–80. [CrossRef]
136. ul Hassan, M.; Emon, A.I.; Luo, F.; Solovyov, V. Design and validation of a 20-kVA, fully cryogenic, two-level GaN-based current source inverter for full electric aircrafts. *IEEE Trans. Transp. Electrif.* **2022**, *8*, 4743–4759. [CrossRef]
137. Wilson, P.R. Advanced aircraft power electronics systems—The impact of simulation, standards and wide band-gap devices. *CES Trans. Electr. Mach. Syst.* **2017**, *1*, 72–82. [CrossRef]
138. Ma, Z.; Liu, D.; Yuan, S.; Duan, Z.; Wu, Z. Damage Effects and Mechanisms of High-Power Microwaves on Double Heterojunction GaN HEMT. *Aerospace* **2024**, *11*, 346. [CrossRef]
139. Galloway, K.F.; Witulski, A.F.; Schrimpf, R.D.; Sternberg, A.L.; Ball, D.R.; Javanainen, A.; Reed, R.A.; Sierawski, B.D.; Lauenstein, J.M. Failure estimates for SiC power MOSFETs in space electronics. *Aerospace* **2018**, *5*, 67. [CrossRef]
140. Arrizabalaga, A.; Álvarez, G. Technical specification envelope for SiC semiconductors to enable high-power in space. *CEAS Space J.* **2024**, 1–12. [CrossRef]
141. Gomez-San-Juan, A.M.; Cubas, J.; Pindado, S. On the thermo-electrical modeling of small satellite's solar panels. *IEEE Trans. Aerosp. Electron. Syst.* **2021**, *57*, 1672–1684. [CrossRef]
142. Propulsion: Lift-Off, Orbit Adjustments and Travelling Through Space. Available online: https://www.esa.int/Enabling-Support/Preparing-for-the-Future/Discovery-and-Preparation/Propulsion-lift-off-orbit-adjustments-and-travelling-through-space (accessed on 25 September 2024).
143. Turan, E.; Speretta, S.; Gill, E. Autonomous navigation for deep space small satellites: Scientific and technological advances. *Acta Astronaut.* **2022**, *193*, 56–74. [CrossRef]
144. Maqsood, M.; Nasir, M.N. Wireless electricity (Power) transmission using solar based power satellite technology. *J. Phys. Conf. Ser.* **2013**, *439*, 012046. [CrossRef]
145. Kulu, E.; Lofqvist, M. Space Solar Power-2023 Survey of Public and Private Initiatives. In Proceedings of the 74th International Astronautical Congress, Baku, Azerbaijan, 2–6 October 2023.
146. Baraskar, A.; Chen, H.; Yoshimura, Y.; Nagasaki, S.; Hanada, T. Verify the wireless power transmission in space using satellite to satellite system. *Int. J. Emerg. Technol.* **2021**, *12*, 110–118.
147. Fusco, F.; Castrillo, V.U.; Giannetta, H.M.R.; Albano, M.; Cavallini, E. Methods, Standards and Components for Wireless Communications and Power Transfer Aimed at Intra-Vehicular Applications of Launchers. *Aerospace* **2024**, *11*, 132. [CrossRef]
148. Lopez, F.; Mauro, A.; Mauro, S.; Monteleone, G.; Sfasciamuro, D.E.; Villa, A. A Lunar-Orbiting Satellite Constellation for Wireless Energy Supply. *Aerospace* **2023**, *10*, 919. [CrossRef]

Disclaimer/Publisher's Note: The statements, opinions and data contained in all publications are solely those of the individual author(s) and contributor(s) and not of MDPI and/or the editor(s). MDPI and/or the editor(s) disclaim responsibility for any injury to people or property resulting from any ideas, methods, instructions or products referred to in the content.